

PRIMAL-DUAL WEAK GALERKIN FINITE ELEMENT METHODS FOR LINEAR CONVECTION EQUATIONS IN NON-DIVERGENCE FORM

DAN LI ^{*}, CHUNMEI WANG [†], AND JUNPING WANG[‡]

Abstract. A new primal-dual weak Galerkin (PD-WG) finite element method was developed and analyzed in this article for first-order linear convection equations in non-divergence form. The PD-WG method results in a symmetric discrete system involving not only the original equation for the primal variable, but also the dual/adjoint equation for the dual variable (also known as Lagrangian multiplier). Optimal order of error estimates in various discrete Sobolev norms are derived for the numerical solutions arising from the PD-WG scheme. Numerical results are produced and reported to illustrate the accuracy and effectiveness of the new PD-WG method.

Key words. primal-dual weak Galerkin, finite element method, weak Galerkin, linear convection equation, discrete weak gradient, polytopal partitions.

AMS subject classifications. Primary, 65N30, 65N15, 65N12; Secondary, 35L02, 35F15, 35B45

1. Introduction. This paper is concerned with the new development of numerical methods for the first-order linear convection equation in non-divergence form. For simplicity, consider the model problem of seeking an unknown function λ satisfying

$$(1.1) \quad \begin{aligned} \boldsymbol{\beta}(x) \cdot \nabla \lambda - c(x)\lambda &= f \quad \text{in } \Omega, \\ \lambda &= g \quad \text{on } \Gamma_-, \end{aligned}$$

where Ω is an open bounded and connected domain in \mathbb{R}^d ($d = 2, 3$) with Lipschitz continuous boundary $\Gamma = \partial\Omega$, Γ_- is the inflow portion of the domain boundary satisfying $\boldsymbol{\beta} \cdot \mathbf{n} < 0$ with \mathbf{n} being the unit outward normal direction to the domain boundary Γ . Assume that the convection vector $\boldsymbol{\beta} = (\beta_1, \dots, \beta_d) \in [L^\infty(\Omega)]^d$, the reaction coefficient $c \in L^\infty(\Omega)$, the load function $f \in L^2(\Omega)$, and the inflow boundary data $g \in L^2(\Gamma_-)$.

The first-order linear partial differential equations (PDEs) of hyperbolic-type are also known as transport equations or linear convection equations which arise in many areas of science and engineering. Readers are referred to the Section of introduction in [8] and the references cited therein for a detailed description of the first-order linear convection equation and some of its physical applications.

This paper aims to develop a new numerical scheme for the linear convection problem (1.1) for which the convection vector $\boldsymbol{\beta}$ and the reaction coefficient c are

^{*}Department of Applied Mathematics, Northwestern Polytechnical University, Xi'an, Shannxi 710072, China.

[†]Department of Mathematics & Statistics, Texas Tech University, Lubbock, TX 79409, USA (chunmei.wang@ttu.edu). The research of Chunmei Wang was partially supported by National Science Foundation Award DMS-1849483.

[‡]Division of Mathematical Sciences, National Science Foundation, Alexandria, VA 22314 (jwang@nsf.gov). The research of Junping Wang was supported in part by the NSF IR/D program, while working at National Science Foundation. However, any opinion, finding, and conclusions or recommendations expressed in this material are those of the author and do not necessarily reflect the views of the National Science Foundation.

assumed to be piecewise smooth functions without any additional coercivity assumption in the form of $c + \frac{1}{2}\nabla \cdot \beta \geq \alpha > 0$ or alike as seen in most existing literatures in the numerical study. Our new numerical scheme will be designed by following the framework of the primal-dual weak Galerkin (PD-WG) finite element method which was introduced and studied in [4, 6, 7, 10, 8, 5]. The PD-WG finite element method was originally formulated as a constraint optimization problem where the optimization is imposed to minimize the “discontinuity” of the approximating functions with the constraint given by a straightforward and local discretization of the underlying PDEs. The resulting Euler-Lagrange formulation gives rise to a symmetric system involving both the primal (original) equation and the dual (adjoint) equation integrated by various stabilizers to provide a certain “weak continuity or smoothness”. It should be noted that the approach of PD-WG finite element method for solving PDEs was also developed by Burman [2, 3] in other finite element contexts, and it was given the name of “*stabilized finite element methods*” by Burman. The recent study has shown that the PD-WG finite element methods have great potentials in numerical PDEs for which the traditional variational formulations are not available or difficult for discretization.

Let us briefly introduce the philosophy of the PD-WG finite element method for solving the first-order linear convection problem (1.1). A weak formulation for the model problem (1.1) is given as follows: Find $\lambda \in H_{\beta}^1(\Omega)$ such that $\lambda = g$ on Γ_- and satisfying

$$(1.2) \quad (\beta \cdot \nabla \lambda - c\lambda, v) = (f, v), \quad \forall v \in L^2(\Omega),$$

where $H_{\beta}^1(\Omega) = \{\lambda \in H^1(\Omega) : \beta \cdot \nabla \lambda \in L^2(\Omega)\}$. The weak gradient operator ∇_w (see [9] for details) can be used to reformulate (1.2) as follows:

$$(1.3) \quad (\beta \cdot \nabla_w \{\lambda\} - c\lambda, v) = (f, v), \quad \forall v \in L^2(\Omega),$$

where $\{\lambda\} = \{\lambda|_T, \lambda|_{\partial T}\}$ is defined as a weak function in the weak Galerkin context. The weak function has approximations by piecewise polynomials on each element T as well as on its boundary ∂T . The weak gradient $\nabla_w \{\lambda\}$ is discretized by using vector-valued polynomials, denoted as $\nabla_{w,h} \{\lambda\}$. The weak formulation (1.3) can then be approximated by seeking $\lambda_h = \{\lambda_0, \lambda_b\} \in W_h$ such that $\lambda_b = Q_b g$ on Γ_- and satisfying

$$(1.4) \quad (\beta \cdot \nabla_{w,h} \lambda_h - c\lambda_0, v) = (f, v), \quad \forall v \in M_h,$$

where W_h is a trial space for the weak functions and M_h is a test space consisting of piecewise polynomials. The problem (1.4) is well-posed if the *inf-sup* condition of Babuška [1] is satisfied. For most readily available trial and test spaces, the *inf-sup* condition of Babuška is difficult to satisfy so that the problem (1.4) is not well posed as it stands. A remedy of this difficulty is to consider the dual equation of (1.4) that seeks $u_h \in M_h$ satisfying

$$(1.5) \quad (\beta \cdot \nabla_{w,h} \sigma - c\sigma, u_h) = 0, \quad \forall \sigma \in W_h^0,$$

where W_h^0 is the subspace of W_h consisting of all weak functions with vanishing boundary values on Γ_- . A formal coupling of (1.4) and (1.5) results in the following primal-dual weak Galerkin scheme: Find $\lambda_h \in W_h$ and $u_h \in M_h$, such that $\lambda_b = Q_b g$

on Γ_- and satisfying

$$(1.6) \quad \begin{cases} s(\lambda_h, \sigma) + (\beta \cdot \nabla_{w,h} \sigma - c\sigma, u_h) = \sum_{T \in \mathcal{T}_h} \tau_1(f, \beta \cdot \nabla \sigma_0 - c\sigma_0), & \forall \sigma \in W_h^0, \\ -\tau_2 \sum_{T \in \mathcal{T}_h} h_T^2(u_h, v)_T + (\beta \cdot \nabla_{w,h} \lambda_h - c\lambda_h, v) = (f, v), & \forall v \in M_h, \end{cases}$$

where $s(\cdot, \cdot)$ is a stabilizer/smooother that enforces a certain weak continuity for the numerical solution λ_h . In fact, the stabilizer aims to measure the level of “continuity” of the weak function $\sigma \in W_h$ in the sense that $\sigma \in W_h$ is a classical C^0 -conforming element if and only if $s(\sigma, \sigma) = 0$.

The linear convection equation (1.1) in non-divergence form is essentially the dual of the model problem in divergence form discussed in [8]. In the development of the PD-WG finite element method in [8], the linear convection equation in divergence form was characterized by a weak form obtained through the usual integration by parts so that no derivatives are taken for the primal unknown. The results are thus of low-regularity assumption as all the derivatives are taken on test functions. For the linear convection equation in non-divergence form (1.1), we shall use a straightforward weak form through a simple test against any square integrable functions. Due to the characterization difference for the primal equations, a least-square term such as $\tau_2 \sum_{T \in \mathcal{T}_h} h_T^2(u_h, v)$ is needed in the primal equation of the new PD-WG scheme (1.6) in order to achieve an optimal order of error estimate in L^2 norm. Furthermore, a term like $\sum_{T \in \mathcal{T}_h} \tau_1(f, \beta \cdot \nabla \sigma_0 - c\sigma_0)$ is added to the right-hand side of the dual equation due to the corresponding least square term in the stabilizer $s(\cdot, \cdot)$. An optimal order error estimate in a discrete Sobolev norm is derived for the new PD-WG scheme of this paper without the development of any *inf-sup* condition, while an *inf-sup* condition was necessary and derived in [8] to establish the optimal order error estimates in various discrete norms. One advantage of this new PD-WG approach compared with the scheme in [8] lies in the fact that polynomials of high degree are employed to approximate the primal variable. More precisely, for the same degree k of polynomials, $P_k(T)$ is used to discretize the primal variable in this paper, while $P_{k-1}(T)$ was employed to approximate the primal variable in [8]. The resulting numerical solutions arising from the PD-WG scheme (1.6) are thus more accurate than those of the PD-WG method in [8] when compared by the same degree of polynomials. The difference is clearly demonstrated by the numerical experiments in each paper.

The paper is organized as follows. Section 2 is devoted to a detailed description of the primal-dual weak Galerkin algorithm for solving the first-order linear convection problem in non-divergence form. The solvability (i.e., the solution existence and uniqueness) of the PD-WG method is shown in Section 3. In Section 4, some error equations for the PD-WG scheme are derived. Section 5 is devoted to the establishment of optimal order error estimates for the PD-WG approximations in some discrete Sobolev norms. In Section 6, an optimal order error estimate in L^2 is derived based on a local H^1 -regularity assumption for the dual problem. In Section 7, some numerical results are reported to demonstrate and verify the effectiveness and accuracy of the new PD-WG method.

Throughout the paper, we follow the usual notation for Sobolev spaces and norms. For any open bounded domain $D \subset \mathbb{R}^d$ (d -dimensional Euclidean space) with Lipschitz continuous boundary, we use $\|\cdot\|_{s,D}$ and $|\cdot|_{s,D}$ to denote the norm and seminorm in

the Sobolev space $H^s(D)$ for any $s \geq 0$, respectively. The inner product in $H^s(D)$ is denoted by $(\cdot, \cdot)_{s,D}$. The space $H^0(D)$ coincides with $L^2(D)$, for which the norm and the inner product are denoted by $\|\cdot\|_D$ and $(\cdot, \cdot)_D$, respectively. When $D = \Omega$, or when the domain of integration is clear from the context, the subscript D is dropped in the norm and inner product notations.

2. Primal-Dual Weak Galerkin Algorithm.

2.1. Discrete weak gradient. Let T be a polygonal or polyhedral domain with boundary ∂T . A weak function on T is defined as a pair $v = \{v_0, v_b\}$ such that $v_0 \in L^2(T)$ and $v_b \in L^2(\partial T)$. The first component v_0 can be viewed as the value of v in the interior of T , while the second component v_b represents v on the boundary of T . In general, v_b may not necessarily be the trace of v_0 on ∂T , though being the trace of v_0 on ∂T would be a viable option for v_b . Denote by $\mathcal{W}(T)$ the local space of all weak functions on T ; i.e.,

$$\mathcal{W}(T) = \{v = \{v_0, v_b\} : v_0 \in L^2(T), v_b \in L^2(\partial T)\}.$$

The weak gradient of $v \in \mathcal{W}(T)$, denoted by $\nabla_w v$, is defined as a linear functional in $[H^1(T)]^d$ such that

$$(\nabla_w v, \boldsymbol{\psi})_T := -(v_0, \nabla \cdot \boldsymbol{\psi})_T + \langle v_b, \boldsymbol{\psi} \cdot \mathbf{n} \rangle_{\partial T}, \quad \forall \boldsymbol{\psi} \in [H^1(T)]^d.$$

Denote by $P_r(T)$ the space of polynomials on T with degree r and less. A discrete version of $\nabla_w v$ for $v \in \mathcal{W}(T)$, denoted as $\nabla_{w,r,T} v$, is defined as the unique polynomial vector in $[P_r(T)]^d$ satisfying

$$(2.1) \quad (\nabla_{w,r,T} v, \boldsymbol{\psi})_T = -(v_0, \nabla \cdot \boldsymbol{\psi})_T + \langle v_b, \boldsymbol{\psi} \cdot \mathbf{n} \rangle_{\partial T}, \quad \forall \boldsymbol{\psi} \in [P_r(T)]^d.$$

From the integration by parts, we may rewrite (2.1) as follows

$$(2.2) \quad (\nabla_{w,r,T} v, \boldsymbol{\psi})_T = (\nabla v_0, \boldsymbol{\psi})_T - \langle v_0 - v_b, \boldsymbol{\psi} \cdot \mathbf{n} \rangle_{\partial T}, \quad \forall \boldsymbol{\psi} \in [P_r(T)]^d,$$

provided that $v_0 \in H^1(T)$.

2.2. Numerical algorithm. Let \mathcal{T}_h be a partition of the domain Ω into polygons in 2D or polyhedra in 3D which is shape regular in the sense of [9]. Denote by \mathcal{E}_h the set of all edges/faces in \mathcal{T}_h , and $\mathcal{E}_h^0 = \mathcal{E}_h \setminus \partial\Omega$ be the set of all interior edges/faces. Denote by h_T the size of $T \in \mathcal{T}_h$ and $h = \max_{T \in \mathcal{T}_h} h_T$ the meshsize of the partition \mathcal{T}_h . For any piecewise smooth function ϕ with respect to the partition \mathcal{T}_h , denote by $[[\phi]]$ the jump of ϕ along the interior edge/face e given by

$$[[\phi]] = \phi_1 \mathbf{n}_1 + \phi_2 \mathbf{n}_2,$$

where $\phi_i := \phi|_{T_i}$, and \mathbf{n}_i is the unit outward normal direction on $e = \partial T_1 \cap \partial T_2$ pointing exterior to the element T_i , $i = 1, 2$.

For any given integer $k \geq 1$, denote by $W_k(T)$ the local space of discrete weak functions; i.e.,

$$W_k(T) = \{\{\sigma_0, \sigma_b\} : \sigma_0 \in P_k(T), \sigma_b \in P_k(e), e \subset \partial T\}.$$

Patching $W_k(T)$ over all the elements $T \in \mathcal{T}_h$ through a common value v_b on the interior interface \mathcal{E}_h^0 , we arrive at a global weak finite element space W_h . Denote by W_h^0 the subspace of W_h with vanishing boundary values on Γ_- ; i.e.,

$$W_h^0 = \{\{\sigma_0, \sigma_b\} \in W_h : \sigma_b|_e = 0, e \subset \Gamma_-\}.$$

Next, let M_h be the finite element space of piecewise polynomials of degree $k-1$; i.e.,

$$M_h = \{w : w|_T \in P_{k-1}(T), \forall T \in \mathcal{T}_h\}.$$

For simplicity of notation and without confusion, for any $\sigma \in W_h$, denote by $\nabla_w \sigma$ the discrete weak gradient $\nabla_{w,k-1,T} \sigma$ computed by (2.1) on each element T ; i.e.,

$$(\nabla_w \sigma)|_T = \nabla_{w,k-1,T}(\sigma|_T), \quad \forall T \in \mathcal{T}_h.$$

In the spaces W_h and M_h , we introduce the following bilinear forms

$$(2.3) \quad \begin{aligned} s(\rho, \sigma) &= \sum_{T \in \mathcal{T}_h} \int_{\partial T} h_T^{-1} (\rho_0 - \rho_b)(\sigma_0 - \sigma_b) ds \\ &\quad + \tau_1 \int_T (\beta \cdot \nabla \rho_0 - c \rho_0)(\beta \cdot \nabla \sigma_0 - c \sigma_0) dT, \\ b(\sigma, v) &= \sum_{T \in \mathcal{T}_h} (\beta \cdot \nabla_w \sigma - c \sigma_0, v)_T, \end{aligned}$$

where $\rho, \sigma \in W_h$, $v \in M_h$, and $\tau_1 \geq 0$ is a parameter.

We are now in a position to state the numerical scheme for the first-order linear convection problem (1.1) in the framework of primal-dual weak Galerkin as follows:

PRIMAL-DUAL WEAK GALERKIN ALGORITHM 2.1. Find $(\lambda_h, u_h) \in W_h \times M_h$, such that $\lambda_b|_e = Q_b(g|_e)$ for all edge/face $e \subset \Gamma_-$ and satisfying

$$(2.4) \quad s(\lambda_h, \sigma) + b(\sigma, u_h) = \sum_{T \in \mathcal{T}_h} \tau_1 (f, \beta \cdot \nabla \sigma_0 - c \sigma_0)_T, \quad \forall \sigma \in W_h^0,$$

$$(2.5) \quad -\tau_2 \sum_{T \in \mathcal{T}_h} h_T^2 (u_h, v)_T + b(\lambda_h, v) = (f, v), \quad \forall v \in M_h,$$

where $\tau_2 > 0$ is a parameter and Q_b is the local L^2 projection operator into $P_k(e)$.

3. Solution Existence and Uniqueness. On each element $T \in \mathcal{T}_h$, let Q_0 be the L^2 projection onto $P_k(T)$, where $k \geq 1$ is any given integer. On each edge/face $e \subset \partial T$, let Q_b be the L^2 projection operator onto $P_k(e)$. For any $w \in H^1(\Omega)$, denote by $Q_h w$ the L^2 projection into the weak finite element space W_h such that

$$(Q_h w)|_T := \{Q_0(w|_T), Q_b(w|_{\partial T})\}, \quad \forall T \in \mathcal{T}_h.$$

Denote by \mathcal{Q}_h the L^2 projection operator onto the finite element space M_h .

LEMMA 3.1. [9] The L^2 projection operators Q_h and \mathcal{Q}_h satisfy the following commutative property:

$$(3.1) \quad \nabla_w(Q_h w) = \mathcal{Q}_h(\nabla w), \quad \forall w \in H^1(T).$$

For simplicity of analysis, assume that the convection vector β and the reaction coefficient c are piecewise smooth functions with respect to the finite element partition \mathcal{T}_h in the rest of the paper.

THEOREM 3.2. *Assume that the first-order linear convection problem (1.1) has a unique solution. The primal-dual weak Galerkin algorithm (2.4)-(2.5) has a unique solution for any parameter $\tau_1 > 0$.*

Proof. It suffices to show that the homogeneous problem of (2.4)-(2.5) has only the trivial solution. To this end, assume $f = 0$ and $g = 0$. By choosing $v = u_h$ and $\sigma = \lambda_h$ in (2.4)-(2.5) we arrive at

$$s(\lambda_h, \lambda_h) + \tau_2 \sum_{T \in \mathcal{T}_h} h_T^2 (u_h, u_h)_T = 0,$$

which implies $\lambda_0 = \lambda_b$ on each ∂T , $\beta \cdot \nabla \lambda_0 - c \lambda_0 = 0$, and $u_h = 0$ on each element T . We thus obtain $\lambda_0 \in C^0(\Omega)$ and furthermore $\beta \cdot \nabla \lambda_0 - c \lambda_0 = 0$ in Ω , which, together with $\lambda_0 = \lambda_b = 0$ on Γ_- , yields $\lambda_0 \equiv 0$ in Ω from the solution uniqueness of the model problem (1.1). From $\lambda_0 = \lambda_b$ on each ∂T , we have $\lambda_b \equiv 0$ in Ω so that $\lambda_h \equiv 0$ in Ω . Additionally, it follows from $u_h \in M_h$ and $u_h = 0$ on each element T that $u_h \equiv 0$ in Ω . This completes the proof of the theorem. \square

The first-order linear convection problem (1.1) with homogeneous boundary condition (i.e., $g = 0$) is said to satisfy a local H^1 -regularity assumption if there exists a non-overlapping partition of the domain $\Omega = \bigcup_{i=1}^J \Omega_i$ such that the solution λ exists, $\lambda|_{\Omega_i} \in H^1(\Omega_i)$ for $i = 1, \dots, J$, and

$$(3.2) \quad \left(\sum_{i=1}^J \|\lambda\|_{1, \Omega_i}^2 \right)^{\frac{1}{2}} \leq C \|f\|,$$

where C is a generic constant.

THEOREM 3.3. *The primal-dual weak Galerkin algorithm (2.4)-(2.5) has a unique solution when the parameter $\tau_1 = 0$ is taken, provided that the meshsize h is sufficiently small such that $h < h_0$ for a fixed but sufficiently small h_0 .*

Proof. It suffices to show that the homogeneous problem of (2.4)-(2.5) has only the trivial solution. To this end, assume $f = 0$ and $g = 0$. As $\tau_1 = 0$, by choosing $v = u_h$ and $\sigma = \lambda_h$ in (2.4)-(2.5) we arrive at

$$s(\lambda_h, \lambda_h) + \tau_2 \sum_{T \in \mathcal{T}_h} h_T^2 (u_h, u_h)_T = 0,$$

which leads to $\lambda_0 = \lambda_b$ on each ∂T and $u_h = 0$ on each element $T \in \mathcal{T}_h$. It follows from (2.5) that

$$\begin{aligned} 0 &= b(\lambda_h, v) \\ &= \sum_{T \in \mathcal{T}_h} (\beta \cdot \nabla_w \lambda_h - c \lambda_0, v)_T \\ &= \sum_{T \in \mathcal{T}_h} (\beta \cdot \nabla \lambda_0 - c \lambda_0, v)_T \\ &= \sum_{T \in \mathcal{T}_h} (\mathcal{Q}_h(\beta \cdot \nabla \lambda_0 - c \lambda_0), v)_T \end{aligned}$$

for all $v \in M_h$, where we have used $\nabla_w \lambda_h = \nabla \lambda_0$ due to the fact that $\lambda_0 = \lambda_b$ on each ∂T plus the identity (2.2). Therefore, we obtain $\mathcal{Q}_h(\beta \cdot \nabla \lambda_0 - c\lambda_0) = 0$ on each $T \in \mathcal{T}_h$ by letting $v = \mathcal{Q}_h(\beta \cdot \nabla \lambda_0 - c\lambda_0) \in M_h$. From $\lambda_0 = \lambda_b$ on each ∂T we have $\lambda \in C^0(\Omega)$. Thus,

$$(3.3) \quad \beta \cdot \nabla \lambda_0 - c\lambda_0 = (I - \mathcal{Q}_h)(\beta \cdot \nabla \lambda_0 - c\lambda_0) := F, \quad \lambda_0|_{\Gamma_-} = 0.$$

Note that the convection coefficient β is piecewise smooth with respect to the partition \mathcal{T}_h . Thus, from the regularity assumption (3.2), the estimate (5.5) with $m = 1$ and $m = 0$, the inverse inequality, and the equation (3.3), we obtain

$$\begin{aligned} \left(\sum_{i=1}^J \|\lambda_0\|_{1,\Omega_i}^2 \right)^{\frac{1}{2}} &\leq C \|F\| \\ &\leq C \|(I - \mathcal{Q}_h)(\beta \cdot \nabla \lambda_0 - c\lambda_0)\| \\ &\leq C \|(I - \mathcal{Q}_h)((\beta - \bar{\beta}) \cdot \nabla \lambda_0)\| + C \|(I - \mathcal{Q}_h)(c\lambda_0)\| \\ &\leq Ch \left(\sum_{T \in \mathcal{T}_h} \|(\beta - \bar{\beta}) \nabla \lambda_0\|_{1,T}^2 + \|c\lambda_0\|_{1,T}^2 \right)^{\frac{1}{2}} \\ &\leq Ch \left(\sum_{T \in \mathcal{T}_h} \|\nabla \lambda_0\|_{0,T}^2 + \|\lambda_0\|_{1,T}^2 \right)^{\frac{1}{2}} \\ &\leq Ch \left(\sum_{i=1}^J \|\lambda_0\|_{1,\Omega_i}^2 \right)^{\frac{1}{2}}, \end{aligned}$$

where $\bar{\beta}$ is the average of β on the element $T \in \mathcal{T}_h$ satisfying the estimate $\|\beta - \bar{\beta}\|_{L^\infty(T)} \leq Ch_T$. Thus, we have

$$(1 - Ch^2) \sum_{i=1}^J \|\lambda_0\|_{1,\Omega_i}^2 \leq 0,$$

which leads to $\lambda_0 \equiv 0$ in Ω_i , $i = 1, \dots, J$, provided that the mesh size h is sufficiently small such that $1 - Ch^2 > 0$. This shows that $\lambda_0 \equiv 0$ in Ω , and furthermore, $\lambda_b \equiv 0$ from the fact that $\lambda_b = \lambda_0$ on each ∂T . This completes the proof of the theorem. \square

4. Error Equations. Let λ be the exact solution of the first-order linear convection problem (1.1) and $(\lambda_h, u_h) \in W_h \times M_h$ be its numerical approximation arising from the scheme (2.4)-(2.5). We define the following two error functions

$$(4.1) \quad \epsilon_h = \lambda_h - \mathcal{Q}_h \lambda,$$

$$(4.2) \quad e_h = u_h - \mathcal{Q}_h u = u_h.$$

Note that the exact solution to the dual equation is the trivial function $u = 0$.

LEMMA 4.1. *The error functions ϵ_h and e_h given in (4.1)-(4.2) satisfy the following error equations:*

$$(4.3) \quad s(\epsilon_h, \sigma) + b(\sigma, e_h) = \ell_\lambda(\sigma), \quad \forall \sigma \in W_h^0,$$

$$(4.4) \quad -\tau_2 \sum_{T \in \mathcal{T}_h} h_T^2 (e_h, v)_T + b(\epsilon_h, v) = \zeta_\lambda(v), \quad \forall v \in M_h.$$

Here,

$$(4.5) \quad \begin{aligned} \ell_\lambda(\sigma) &= \sum_{T \in \mathcal{T}_h} \tau_1 (\boldsymbol{\beta} \cdot \nabla (\lambda - Q_0 \lambda) - c(\lambda - Q_0 \lambda), \boldsymbol{\beta} \cdot \nabla \sigma_0 - c\sigma_0)_T \\ &\quad - h_T^{-1} \langle Q_0 \lambda - Q_b \lambda, \sigma_0 - \sigma_b \rangle_{\partial T}, \end{aligned}$$

$$(4.6) \quad \zeta_\lambda(v) = \sum_{T \in \mathcal{T}_h} (\boldsymbol{\beta} \cdot (I - \mathcal{Q}_h) \nabla \lambda - c(\lambda - Q_0 \lambda), v)_T.$$

Proof. From (2.5) and the commutative property (3.1) we have

$$\begin{aligned} & -\tau_2 \sum_{T \in \mathcal{T}_h} h_T^2 (u_h - \mathcal{Q}_h u, v)_T + b(\lambda_h - Q_h \lambda, v) \\ &= (f, v) - b(Q_h \lambda, v) \\ &= (f, v) - \sum_{T \in \mathcal{T}_h} (\boldsymbol{\beta} \cdot \nabla_w Q_h \lambda - cQ_0 \lambda, v)_T \\ &= (\boldsymbol{\beta} \cdot \nabla \lambda - c\lambda, v) - \sum_{T \in \mathcal{T}_h} (\boldsymbol{\beta} \cdot \mathcal{Q}_h \nabla \lambda - cQ_0 \lambda, v)_T \\ &= \sum_{T \in \mathcal{T}_h} (\boldsymbol{\beta} \cdot (I - \mathcal{Q}_h) \nabla \lambda - c(\lambda - Q_0 \lambda), v)_T, \end{aligned}$$

where we used the first equation in (1.1), which gives (4.4). To derive (4.3), we subtract $s(Q_h \lambda, \sigma)$ from both sides of (2.4) to obtain

$$\begin{aligned} & s(\lambda_h - Q_h \lambda, \sigma) + b(\sigma, u_h - \mathcal{Q}_h u) \\ &= \sum_{T \in \mathcal{T}_h} \tau_1 (f, \boldsymbol{\beta} \cdot \nabla \sigma_0 - c\sigma_0)_T - s(Q_h \lambda, \sigma) \\ &= \sum_{T \in \mathcal{T}_h} \tau_1 (\boldsymbol{\beta} \cdot \nabla \lambda - c\lambda, \boldsymbol{\beta} \cdot \nabla \sigma_0 - c\sigma_0)_T - h_T^{-1} \langle Q_0 \lambda - Q_b \lambda, \sigma_0 - \sigma_b \rangle_{\partial T} \\ &\quad - \tau_1 (\boldsymbol{\beta} \cdot \nabla Q_0 \lambda - cQ_0 \lambda, \boldsymbol{\beta} \cdot \nabla \sigma_0 - c\sigma_0)_T \\ &= \sum_{T \in \mathcal{T}_h} \tau_1 (\boldsymbol{\beta} \cdot \nabla (\lambda - Q_0 \lambda) - c(\lambda - Q_0 \lambda), \boldsymbol{\beta} \cdot \nabla \sigma_0 - c\sigma_0)_T \\ &\quad - h_T^{-1} \langle Q_0 \lambda - Q_b \lambda, \sigma_0 - \sigma_b \rangle_{\partial T}, \end{aligned}$$

which verifies the error equation (4.3). This completes the proof of the lemma. \square

5. Error Estimates. We first introduce a scaled L^2 norm in the finite element space M_h as follows:

$$(5.1) \quad \|v\|_{M_h} = \left(\tau_2 \sum_{T \in \mathcal{T}_h} h_T^2 \|v\|_T^2 \right)^{\frac{1}{2}}, \quad v \in M_h,$$

where $\tau_2 > 0$ is a given parameter. Next, we introduce a semi-norm in the weak finite element space W_h :

$$(5.2) \quad \|\lambda\|_{W_h} = \left(\sum_{T \in \mathcal{T}_h} h_T^{-1} \|\lambda_0 - \lambda_b\|_{\partial T}^2 + \tau_1 \|\boldsymbol{\beta} \cdot \nabla \lambda_0 - c\lambda_0\|_T^2 \right)^{\frac{1}{2}},$$

where $\tau_1 \geq 0$ is another parameter.

LEMMA 5.1. *Assume that the solution to the first-order linear convection problem in the non-divergence form (1.1) is unique. Then the seminorm $\|\cdot\|_{W_h}$ given in (5.2) defines a norm in the linear space W_h^0 for any given $\tau_1 > 0$.*

Proof. We shall only verify the positivity property for $\|\cdot\|_{W_h}$. To this end, assume $\|\lambda\|_{W_h} = 0$ for some $\lambda = \{\lambda_0, \lambda_b\} \in W_h^0$. Since $\tau_1 > 0$, then from (5.2) we have $\lambda_0 = \lambda_b$ on ∂T and $\beta \cdot \nabla \lambda_0 - c\lambda_0 = 0$ on any $T \in \mathcal{T}_h$. This implies $\lambda_0 \in C^0(\Omega)$ and $\beta \cdot \nabla \lambda_0 - c\lambda_0 = 0$ in Ω . Thus, from $\lambda \in W_h^0$ and the solution uniqueness for the first-order linear convection problem (1.1) we obtain $\lambda_0 \equiv 0$ and furthermore, $\lambda_b = \lambda_0 = 0$. This completes the proof of the lemma. \square

Recall that \mathcal{T}_h is a shape-regular finite element partition of the domain Ω . Thus, for any $T \in \mathcal{T}_h$ and $\phi \in H^1(T)$, the following trace inequality holds true [9]:

$$(5.3) \quad \|\phi\|_{\partial T}^2 \leq C(h_T^{-1}\|\phi\|_T^2 + h_T\|\nabla\phi\|_T^2).$$

If ϕ is a polynomial on the element $T \in \mathcal{T}_h$, the following trace inequality holds true [9]; i.e.,

$$(5.4) \quad \|\phi\|_{\partial T}^2 \leq Ch_T^{-1}\|\phi\|_T^2.$$

LEMMA 5.2. [9] *Let \mathcal{T}_h be a finite element partition of the domain Ω satisfying the shape regular assumption as specified in [9]. For any $0 \leq s \leq 1$ and $0 \leq m \leq k$, there holds*

$$(5.5) \quad \sum_{T \in \mathcal{T}_h} h_T^{2s} \|u - \mathcal{Q}_h u\|_{s,T}^2 \leq Ch^{2m} \|u\|_m^2,$$

$$(5.6) \quad \sum_{T \in \mathcal{T}_h} h_T^{2s} \|\lambda - \mathcal{Q}_0 \lambda\|_{s,T}^2 \leq Ch^{2m+2} \|\lambda\|_{m+1}^2.$$

THEOREM 5.3. *Let λ and $(\lambda_h; u_h) \in W_h \times M_h$ be the exact solution of the first-order linear convection problem (1.1) and the primal-dual weak Galerkin solution arising from the numerical scheme (2.4)-(2.5), respectively. Assume that the exact solution λ is sufficiently regular such that $\lambda \in \oplus_{i=1}^J H^{k+1}(\Omega_i)$ where $\{\Omega_i\}_{i=1}^J$ is a non-overlapping partition of the domain Ω . There exists a constant C such that*

$$(5.7) \quad \|\epsilon_h\|_{W_h} + \|e_h\|_{M_h} \leq C(1 + \tau_2^{-\frac{1}{2}})h^k \|\lambda\|_{k+1}.$$

Proof. By setting $\sigma = \epsilon_h$ in the error equation (4.3) and $v = e_h$ in (4.4), we have from the resulting (4.3) and (4.4) that

$$\tau_2 \sum_{T \in \mathcal{T}_h} h_T^2 (e_h, e_h)_T + s(\epsilon_h, \epsilon_h) = \ell_\lambda(\epsilon_h) - \zeta_\lambda(e_h),$$

which gives

$$(5.8) \quad \|e_h\|_{M_h}^2 + \|\epsilon_h\|_{W_h}^2 \leq |\ell_\lambda(\epsilon_h)| + |\zeta_\lambda(e_h)| = I_1 + I_2.$$

We shall estimate the two terms I_1 and I_2 in (5.8). For the term I_1 , it follows from the Cauchy-Schwarz inequality, the triangle inequality, (4.5), the trace inequality (5.3), and the estimate (5.6) with $m = k$ that

$$\begin{aligned}
(5.9) \quad I_1 &= \left| \sum_{T \in \mathcal{T}_h} \tau_1 (\boldsymbol{\beta} \cdot \nabla (\lambda - Q_0 \lambda) - c(\lambda - Q_0 \lambda), \boldsymbol{\beta} \cdot \nabla \epsilon_0 - c\epsilon_0)_T \right. \\
&\quad \left. - h_T^{-1} \langle Q_0 \lambda - Q_b \lambda, \epsilon_0 - \epsilon_b \rangle_{\partial T} \right| \\
&\leq \left(\left(\sum_{T \in \mathcal{T}_h} \tau_1 \|\boldsymbol{\beta} \cdot \nabla (\lambda - Q_0 \lambda)\|_T^2 \right)^{\frac{1}{2}} + \left(\sum_{T \in \mathcal{T}_h} \tau_1 \|c(\lambda - Q_0 \lambda)\|_T^2 \right)^{\frac{1}{2}} \right) \\
&\quad \cdot \left(\sum_{T \in \mathcal{T}_h} \tau_1 \|\boldsymbol{\beta} \cdot \nabla \epsilon_0 - c\epsilon_0\|_T^2 \right)^{\frac{1}{2}} \\
&\quad + \left(\sum_{T \in \mathcal{T}_h} h_T^{-1} \|\epsilon_0 - \epsilon_b\|_{\partial T}^2 \right)^{\frac{1}{2}} \left(\sum_{T \in \mathcal{T}_h} h_T^{-1} \|Q_0 \lambda - Q_b \lambda\|_{\partial T}^2 \right)^{\frac{1}{2}} \\
&\leq \|\epsilon_h\|_{W_h} (Ch^k \|\lambda\|_{k+1} + Ch^{k+1} \|\lambda\|_{k+1}) \\
&\quad + \|\epsilon_h\|_{W_h} \left(\sum_{T \in \mathcal{T}_h} h_T^{-1} \|Q_0 \lambda - \lambda\|_{\partial T}^2 \right)^{\frac{1}{2}} \\
&\leq \|\epsilon_h\|_{W_h} \left(Ch^k \|\lambda\|_{k+1} + C \left(\sum_{T \in \mathcal{T}_h} h_T^{-2} \|Q_0 \lambda - \lambda\|_T^2 + \|Q_0 \lambda - \lambda\|_{1,T}^2 \right)^{\frac{1}{2}} \right) \\
&\leq Ch^k \|\epsilon_h\|_{W_h} \|\lambda\|_{k+1}.
\end{aligned}$$

As to term I_2 , we use the orthogonality property of \mathcal{Q}_h to obtain

$$\begin{aligned}
I_2 &= \left| \sum_{T \in \mathcal{T}_h} (\boldsymbol{\beta} \cdot (I - \mathcal{Q}_h) \nabla \lambda - c(\lambda - Q_0 \lambda), e_h)_T \right| \\
&\leq \left| \sum_{T \in \mathcal{T}_h} (\boldsymbol{\beta} \cdot (I - \mathcal{Q}_h) \nabla \lambda, e_h)_T \right| + \left| \sum_{T \in \mathcal{T}_h} (c(\lambda - Q_0 \lambda), e_h)_T \right| \\
&= \left| \sum_{T \in \mathcal{T}_h} ((I - \mathcal{Q}_h) \nabla \lambda, (I - \mathcal{Q}_h)(\boldsymbol{\beta} - \bar{\boldsymbol{\beta}})e_h)_T \right| \\
&\quad + \left| \sum_{T \in \mathcal{T}_h} (\lambda - Q_0 \lambda, ce_h)_T \right|.
\end{aligned}$$

Next, from the Cauchy-Schwarz inequality, (4.6), the triangle inequality, the estimate (5.5) with $m = k$ and $m = 1$, the estimate (5.6) with $m = k$, and the inverse inequality we obtain

$$\begin{aligned}
|I_2| &\leq \left(\sum_{T \in \mathcal{T}_h} \|(I - \mathcal{Q}_h) \nabla \lambda\|_T^2 \right)^{\frac{1}{2}} \left(\sum_{T \in \mathcal{T}_h} \|(I - \mathcal{Q}_h)(\beta - \bar{\beta})e_h\|_T^2 \right)^{\frac{1}{2}} \\
&\quad + \|c\|_{L^\infty(\Omega)} \left(\sum_{T \in \mathcal{T}_h} \tau_2^{-1} h_T^{-2} \|Q_0 \lambda - \lambda\|_T^2 \right)^{\frac{1}{2}} \left(\sum_{T \in \mathcal{T}_h} \tau_2 h_T^2 \|e_h\|_T^2 \right)^{\frac{1}{2}} \\
&\leq Ch^k \|\lambda\|_{k+1} \left(\sum_{T \in \mathcal{T}_h} h_T^2 \|(\beta - \bar{\beta})e_h\|_{1,T}^2 \right)^{\frac{1}{2}} + C\tau_2^{-\frac{1}{2}} h^k \|\lambda\|_{k+1} \|e_h\|_{M_h} \\
(5.10) \quad &\leq Ch^k \|\lambda\|_{k+1} \left(\sum_{T \in \mathcal{T}_h} h_T^2 (\|e_h \nabla \beta\|_T^2 + \|(\beta - \bar{\beta}) \cdot \nabla e_h\|_T^2) \right)^{\frac{1}{2}} \\
&\quad + C\tau_2^{-\frac{1}{2}} h^k \|\lambda\|_{k+1} \|e_h\|_{M_h} \\
&\leq C\tau_2^{-\frac{1}{2}} h^k \|\lambda\|_{k+1} \left(\sum_{T \in \mathcal{T}_h} \tau_2 h_T^2 (\|e_h\|_T^2 + h_T^2 h_T^{-2} \|e_h\|_T^2) \right)^{\frac{1}{2}} \\
&\quad + C\tau_2^{-\frac{1}{2}} h^k \|\lambda\|_{k+1} \|e_h\|_{M_h} \\
&\leq C\tau_2^{-\frac{1}{2}} h^k \|\lambda\|_{k+1} \|e_h\|_{M_h},
\end{aligned}$$

where $\bar{\beta}$ is the average of β on each $T \in \mathcal{T}_h$ satisfying $\|\beta - \bar{\beta}\|_{L^\infty(T)} \leq Ch_T$. Combining (5.8) with (5.9) and (5.10) yields the error estimate (5.7). This completes the proof of the theorem. \square

6. Error Estimates in L^2 . For any $\theta \in L^2(\Omega)$, consider the auxiliary problem of seeking an unknown function w satisfying

$$(6.1) \quad -\nabla \cdot (\beta w) - cw = \theta, \quad \text{in } \Omega,$$

$$(6.2) \quad w = 0, \quad \text{on } \Gamma_+,$$

where $\Gamma_+ = \partial\Omega \setminus \Gamma_-$ is the outflow boundary satisfying $\beta \cdot \mathbf{n} \geq 0$ with \mathbf{n} being the unit outward normal direction to $\partial\Omega$. The problem (6.1)-(6.2) is said to satisfy a local H^1 -regularity assumption if there exists a non-overlapping partition of the domain $\Omega = \bigcup_{i=1}^J \Omega_i$ such that there exists a solution w , $w \in H^1(\Omega_i)$ for $i = 1, \dots, J$, satisfying

$$(6.3) \quad \left(\sum_{i=1}^J \|w\|_{1,\Omega_i}^2 \right)^{\frac{1}{2}} \leq C \|\theta\|,$$

where C is a generic constant.

LEMMA 6.1. *For any $\sigma = \{\sigma_0, \sigma_b\} \in W_k(T)$, there holds*

$$(6.4) \quad \|\nabla_w \sigma\|_T^2 \leq C \left(\|\nabla \sigma_0\|_T^2 + s_T(\sigma, \sigma) \right),$$

where C is a constant independent of $T \in \mathcal{T}_h$.

Proof. It follows from (2.2), the Cauchy-Schwarz inequality, the triangle inequality, and the trace inequality (5.4) that

$$\begin{aligned}
|(\nabla_w \sigma, \varphi)_T| &= |(\nabla \sigma_0, \varphi)_T - \langle \sigma_0 - \sigma_b, \varphi \cdot \mathbf{n} \rangle_{\partial T}| \\
&\leq |(\nabla \sigma_0, \varphi)_T| + |\langle \sigma_0 - \sigma_b, \varphi \cdot \mathbf{n} \rangle_{\partial T}| \\
&\leq \|\nabla \sigma_0\|_T \|\varphi\|_T + \|\sigma_0 - \sigma_b\|_{\partial T} \|\varphi \cdot \mathbf{n}\|_{\partial T} \\
&\leq \left(\|\nabla \sigma_0\|_T + Ch_T^{-\frac{1}{2}} \|\sigma_b - \sigma_0\|_{\partial T} \right) \|\varphi\|_T,
\end{aligned}$$

for any $\varphi \in [P_{k-1}(T)]^d$, which implies

$$\|\nabla_w \sigma\|_T^2 \leq C \left(\|\nabla \sigma_0\|_T^2 + h_T^{-1} \|\sigma_b - \sigma_0\|_{\partial T}^2 \right).$$

This completes the proof of the lemma. \square

LEMMA 6.2. For any $\sigma = \{\sigma_0, \sigma_b\} \in W_h^0$, the following identity holds true

$$(6.5) \quad (\sigma_0, \theta) = \sum_{T \in \mathcal{T}_h} (\beta \cdot \nabla_w \sigma - c\sigma_0, w)_T + \langle \sigma_0 - \sigma_b, (\mathcal{Q}_h - I)(\beta w) \cdot \mathbf{n} \rangle_{\partial T}.$$

Proof. From testing (6.1) with σ_0 on each element $T \in \mathcal{T}_h$, and then using the integration by parts we have

$$\begin{aligned}
(\sigma_0, \theta) &= \sum_{T \in \mathcal{T}_h} (-\nabla \cdot (\beta w) - cw, \sigma_0)_T \\
(6.6) \quad &= \sum_{T \in \mathcal{T}_h} (w, \beta \cdot \nabla \sigma_0 - c\sigma_0)_T - \langle \beta w \cdot \mathbf{n}, \sigma_0 \rangle_{\partial T} \\
&= \sum_{T \in \mathcal{T}_h} (w, \beta \cdot \nabla \sigma_0 - c\sigma_0)_T - \langle \beta w \cdot \mathbf{n}, \sigma_0 - \sigma_b \rangle_{\partial T},
\end{aligned}$$

where we have used the homogeneous boundary condition (6.2) and $\sigma_b = 0$ on Γ_- in the last line.

Next, by setting $\varphi = \mathcal{Q}_h(\beta w)$ in (2.2), we have

$$\begin{aligned}
(\nabla_w \sigma, \mathcal{Q}_h(\beta w))_T &= (\nabla \sigma_0, \mathcal{Q}_h(\beta w))_T - \langle \sigma_0 - \sigma_b, \mathcal{Q}_h(\beta w) \cdot \mathbf{n} \rangle_{\partial T} \\
&= (\nabla \sigma_0, \beta w)_T - \langle \sigma_0 - \sigma_b, \mathcal{Q}_h(\beta w) \cdot \mathbf{n} \rangle_{\partial T},
\end{aligned}$$

which leads to

$$\begin{aligned}
(6.7) \quad (\beta \cdot \nabla \sigma_0, w)_T &= (\nabla_w \sigma, \mathcal{Q}_h(\beta w))_T + \langle \sigma_0 - \sigma_b, \mathcal{Q}_h(\beta w) \cdot \mathbf{n} \rangle_{\partial T} \\
&= (\nabla_w \sigma, \beta w)_T + \langle \sigma_0 - \sigma_b, \mathcal{Q}_h(\beta w) \cdot \mathbf{n} \rangle_{\partial T}.
\end{aligned}$$

Substituting (6.7) into (6.6) yields

$$(\sigma_0, \theta) = \sum_{T \in \mathcal{T}_h} (\beta \cdot \nabla_w \sigma - c\sigma_0, w)_T + \langle \sigma_0 - \sigma_b, (\mathcal{Q}_h - I)(\beta w) \cdot \mathbf{n} \rangle_{\partial T},$$

which completes the proof of the lemma. \square

The following lemma is devoted to an estimate for the second term on the right-hand side of (6.5) based on the local H^1 -regularity assumption (6.3) for the auxiliary problem (6.1)-(6.2).

LEMMA 6.3. *Assume that the auxiliary problem (6.1)-(6.2) satisfies the local H^1 -regularity assumption (6.3). Then, for any $\sigma \in W_h^0$, there holds*

$$(6.8) \quad \left| \sum_{T \in \mathcal{T}_h} \langle \sigma_0 - \sigma_b, (\mathcal{Q}_h - I)(\beta w) \cdot \mathbf{n} \rangle_{\partial T} \right| \leq Ch \|\theta\| \|\sigma\|_{W_h}.$$

Proof. From the Cauchy-Schwarz inequality, the trace inequality (5.3), the local H^1 -regularity (6.3), and the estimate (5.5) with $m = 1$, we have

$$\begin{aligned} & \left| \sum_{T \in \mathcal{T}_h} \langle \sigma_0 - \sigma_b, (\mathcal{Q}_h - I)(\beta w) \cdot \mathbf{n} \rangle_{\partial T} \right| \\ & \leq \left(\sum_{T \in \mathcal{T}_h} h_T^{-1} \|\sigma_0 - \sigma_b\|_{\partial T}^2 \right)^{\frac{1}{2}} \left(\sum_{T \in \mathcal{T}_h} h_T \|(\mathcal{Q}_h - I)(\beta w) \cdot \mathbf{n}\|_{\partial T}^2 \right)^{\frac{1}{2}} \\ & \leq C \|\sigma\|_{W_h} \left(\sum_{T \in \mathcal{T}_h} \|(\mathcal{Q}_h - I)(\beta w)\|_T^2 + h_T^2 \|(\mathcal{Q}_h - I)(\beta w)\|_{1,T}^2 \right)^{\frac{1}{2}} \\ & \leq C \|\sigma\|_{W_h} \left(\sum_{i=1}^J h^2 \|w\|_{1,\Omega_i}^2 \right)^{\frac{1}{2}} \\ & \leq Ch \|\theta\| \|\sigma\|_{W_h}, \end{aligned}$$

which completes the proof of the lemma. \square

The following is an error estimate in the usual L^2 norm for the first component λ_0 of the primal variable λ_h .

THEOREM 6.4. *Let $\lambda_h = \{\lambda_0, \lambda_b\} \in W_h$ be the primal-dual weak Galerkin solution arising from the PD-WG scheme (2.4)-(2.5) with $u_h \in M_h$ being the numerical Lagrangian multiplier. Assume that the exact solution λ of the first-order linear convection model problem (1.1) is sufficiently regular such that $\lambda \in H^{k+1}(\Omega)$. Under the local H^1 -regularity assumption (6.3) for the auxiliary problem (6.1)-(6.2), there holds*

$$(6.9) \quad \|\epsilon_0\|_0 \leq C(1 + (h + 1 + \tau_2^{\frac{1}{2}})(1 + \tau_2^{-\frac{1}{2}}))h^{k+1}\|\lambda\|_{k+1},$$

provided that the meshsize h is sufficiently small such that $h < h_0$ for a fixed but sufficiently small h_0 .

Proof. Let w be the solution of the auxiliary problem (6.1)-(6.2) for a given function θ . By setting $\sigma = \epsilon_h \in W_h^0$ in Lemma 6.2 we obtain

$$\begin{aligned} (6.10) \quad (\epsilon_0, \theta) &= \sum_{T \in \mathcal{T}_h} (\beta \cdot \nabla_w \epsilon_h - c \epsilon_0, w)_T + \sum_{T \in \mathcal{T}_h} \langle \epsilon_0 - \epsilon_b, (\mathcal{Q}_h - I)(\beta w) \cdot \mathbf{n} \rangle_{\partial T} \\ &= I_1 + I_2, \end{aligned}$$

where I_1 and I_2 are defined accordingly.

For the term I_2 , we use the estimate in Lemma 6.3 to obtain

$$(6.11) \quad |I_2| \leq Ch \|\theta\| \|\epsilon_h\|_{W_h}.$$

As to the term I_1 , we use the error equation (4.4) to obtain

$$\begin{aligned}
 I_1 &= \sum_{T \in \mathcal{T}_h} (\beta \cdot \nabla_w \epsilon_h - c\epsilon_0, w)_T \\
 &= \sum_{T \in \mathcal{T}_h} (\beta \cdot \nabla_w \epsilon_h - c\epsilon_0, \mathcal{Q}_h w)_T + \sum_{T \in \mathcal{T}_h} (\beta \cdot \nabla_w \epsilon_h - c\epsilon_0, (I - \mathcal{Q}_h)w)_T \\
 (6.12) \quad &= \sum_{T \in \mathcal{T}_h} (\beta \cdot (I - \mathcal{Q}_h) \nabla \lambda, \mathcal{Q}_h w)_T + \sum_{T \in \mathcal{T}_h} (c(Q_0 \lambda - \lambda), \mathcal{Q}_h w)_T \\
 &\quad + \sum_{T \in \mathcal{T}_h} \tau_2 h_T^2 (e_h, \mathcal{Q}_h w)_T + \sum_{T \in \mathcal{T}_h} (\beta \cdot \nabla_w \epsilon_h - c\epsilon_0, (I - \mathcal{Q}_h)w)_T \\
 &= I_{11} + I_{12} + I_{13} + I_{14},
 \end{aligned}$$

where I_{11}, I_{12}, I_{13} , and I_{14} are defined accordingly. We shall estimate the four terms I_{11}, I_{12}, I_{13} , and I_{14} in (6.12) one by one. For the term I_{11} , from the Cauchy-Schwarz inequality, the estimate (5.5) with $m = 1$ and $m = k$, and the regularity assumption (6.3), we have

$$\begin{aligned}
 |I_{11}| &= \left| \sum_{T \in \mathcal{T}_h} (\beta \cdot (I - \mathcal{Q}_h) \nabla \lambda, \mathcal{Q}_h w)_T \right| \\
 &= \left| \sum_{T \in \mathcal{T}_h} ((I - \mathcal{Q}_h) \nabla \lambda, (I - \mathcal{Q}_h) \beta \cdot \mathcal{Q}_h w)_T \right| \\
 (6.13) \quad &= \left(\sum_{T \in \mathcal{T}_h} \|(I - \mathcal{Q}_h) \nabla \lambda\|_T^2 \right)^{\frac{1}{2}} \left(\sum_{T \in \mathcal{T}_h} \|(I - \mathcal{Q}_h) \beta \cdot \mathcal{Q}_h w\|_T^2 \right)^{\frac{1}{2}} \\
 &\leq Ch^{k+1} \|\lambda\|_{k+1} \left(\sum_{i=1}^J \|w\|_{1, \Omega_i}^2 \right)^{\frac{1}{2}} \\
 &\leq Ch^{k+1} \|\lambda\|_{k+1} \|\theta\|.
 \end{aligned}$$

For the term I_{12} , we use the Cauchy-Schwarz inequality, the estimate (5.6) with $m = k$, and the regularity assumption (6.3) to obtain

$$\begin{aligned}
 |I_{12}| &= \left| \sum_{T \in \mathcal{T}_h} (Q_0 \lambda - \lambda, c \mathcal{Q}_h w)_T \right| \\
 &= \left(\sum_{T \in \mathcal{T}_h} \|Q_0 \lambda - \lambda\|_T^2 \right)^{\frac{1}{2}} \left(\sum_{T \in \mathcal{T}_h} \|c \mathcal{Q}_h w\|_T^2 \right)^{\frac{1}{2}} \\
 (6.14) \quad &\leq Ch^{k+1} \|\lambda\|_{k+1} \left(\sum_{i=1}^J \|w\|_{1, \Omega_i}^2 \right)^{\frac{1}{2}} \\
 &\leq Ch^{k+1} \|\lambda\|_{k+1} \|\theta\|.
 \end{aligned}$$

For the term I_{13} , we use the Cauchy-Schwarz inequality, the error estimate (5.7), and

the regularity assumption (6.3) to obtain

$$\begin{aligned}
|I_{13}| &= \left| \sum_{T \in \mathcal{T}_h} \tau_2 h_T^2 (e_h, \mathcal{Q}_h w)_T \right| \\
(6.15) \quad &\leq \left(\sum_{T \in \mathcal{T}_h} \tau_2 h_T^2 \|e_h\|_T^2 \right)^{\frac{1}{2}} \left(\sum_{T \in \mathcal{T}_h} \tau_2 h_T^2 \|\mathcal{Q}_h w\|_T^2 \right)^{\frac{1}{2}} \\
&\leq C \tau_2^{\frac{1}{2}} h \|e_h\|_{M_h} \|w\|_0 \\
&\leq C \tau_2^{\frac{1}{2}} (1 + \tau_2^{-\frac{1}{2}}) h^{k+1} \|\lambda\|_{k+1} \|\theta\|.
\end{aligned}$$

As to the term I_{14} , from the Cauchy-Schwarz inequality, (6.4), the estimate (5.5) with $m = 1$, the inverse inequality, and the regularity assumption (6.3) we have

$$\begin{aligned}
|I_{14}| &= \left| \sum_{T \in \mathcal{T}_h} (\beta \cdot \nabla_w \epsilon_h - c \epsilon_0, (I - \mathcal{Q}_h)w)_T \right| \\
&\leq \left| \sum_{T \in \mathcal{T}_h} ((\beta - \bar{\beta}) \cdot \nabla_w \epsilon_h - c \epsilon_0, (I - \mathcal{Q}_h)w)_T \right| \\
&\leq \left(\left(\sum_{T \in \mathcal{T}_h} \|\beta - \bar{\beta}\|_{L^\infty(T)}^2 \|\nabla_w \epsilon_h\|_T^2 \right)^{\frac{1}{2}} + \|c\|_{L^\infty(\Omega)} \left(\sum_{T \in \mathcal{T}_h} \|\epsilon_0\|_T^2 \right)^{\frac{1}{2}} \right) \\
(6.16) \quad &\cdot \left(\sum_{T \in \mathcal{T}_h} \|(I - \mathcal{Q}_h)w\|_T^2 \right)^{\frac{1}{2}} \\
&\leq \left(\left(\sum_{T \in \mathcal{T}_h} h_T^2 \|\nabla_w \epsilon_h\|_T^2 \right)^{\frac{1}{2}} + C \left(\sum_{T \in \mathcal{T}_h} \|\epsilon_0\|_T^2 \right)^{\frac{1}{2}} \right) Ch \left(\sum_{i=1}^J \|w\|_{1, \Omega_i}^2 \right)^{\frac{1}{2}} \\
&\leq Ch \left(\left(C \sum_{T \in \mathcal{T}_h} h_T^2 \|\nabla \epsilon_0\|_T^2 + h_T^2 s_T(\epsilon_h, \epsilon_h) \right)^{\frac{1}{2}} + C \left(\sum_{T \in \mathcal{T}_h} \|\epsilon_0\|_T^2 \right)^{\frac{1}{2}} \right) \|\theta\| \\
&\leq Ch (C \|\epsilon_0\| + Ch \|\epsilon_h\|_{W_h}) \|\theta\|,
\end{aligned}$$

where $\bar{\beta}$ is the average of β on each element $T \in \mathcal{T}_h$ satisfying $\|\beta - \bar{\beta}\|_{L^\infty(T)} \leq Ch_T$. By substituting (6.13) - (6.16) into (6.12), we obtain the following estimate for the term I_1 :

$$\begin{aligned}
|I_1| &\leq Ch \left(C \|\epsilon_0\| + h \|\epsilon_h\|_{W_h} + (1 + \tau_2^{\frac{1}{2}} (1 + \tau_2^{-\frac{1}{2}})) h^k \|\lambda\|_{k+1} \right) \|\theta\| \\
(6.17) \quad &\leq Ch \left(C \|\epsilon_0\| + (1 + \tau_2^{-\frac{1}{2}}) h^{k+1} \|\lambda\|_{k+1} + (1 + \tau_2^{\frac{1}{2}} (1 + \tau_2^{-\frac{1}{2}})) h^k \|\lambda\|_{k+1} \right) \|\theta\|,
\end{aligned}$$

where we have used the error estimate (5.7).

Substituting (6.17) and (6.11) into (6.10) yields

$$\begin{aligned}
|(\epsilon_0, \theta)| &\leq Ch \left(C \|\epsilon_0\| + (1 + \tau_2^{-\frac{1}{2}}) h^{k+1} \|\lambda\|_{k+1} + (1 + \tau_2^{\frac{1}{2}} (1 + \tau_2^{-\frac{1}{2}})) h^k \|\lambda\|_{k+1} \right) \|\theta\| \\
&\quad + C (1 + \tau_2^{-\frac{1}{2}}) \|\theta\| h^{k+1} \|\lambda\|_{k+1},
\end{aligned}$$

where we used the error estimate (5.7). Since the set of all such θ is dense in $L^2(\Omega)$, the above inequality leads to

$$\begin{aligned}
\|\epsilon_0\| &\leq Ch \left(C \|\epsilon_0\| + (1 + \tau_2^{-\frac{1}{2}}) h^{k+1} \|\lambda\|_{k+1} + (1 + \tau_2^{\frac{1}{2}} (1 + \tau_2^{-\frac{1}{2}})) h^k \|\lambda\|_{k+1} \right) \\
&\quad + C (1 + \tau_2^{-\frac{1}{2}}) h^{k+1} \|\lambda\|_{k+1},
\end{aligned}$$

and furthermore

$$(1 - Ch)\|\epsilon_0\| \leq C(1 + (h + 1 + \tau_2^{\frac{1}{2}})(1 + \tau_2^{-\frac{1}{2}}))h^{k+1}\|\lambda\|_{k+1}.$$

This completes the proof of the theorem provided that the meshsize h is sufficiently small such that $1 - Ch > \frac{1}{2}$. \square

To establish an error estimate for the boundary component λ_b , we introduce the following norm

$$\|\epsilon_b\|_{0,*} := \left(\sum_{T \in \mathcal{T}_h} h_T \|\epsilon_b\|_{\partial T}^2 \right)^{\frac{1}{2}}.$$

THEOREM 6.5. *Under the assumptions of Theorem 6.4, there holds*

$$\|\epsilon_b\|_{0,*} \leq C(1 + (h + 1 + \tau_2^{\frac{1}{2}})(1 + \tau_2^{-\frac{1}{2}}))h^{k+1}\|\lambda\|_{k+1}.$$

Proof. On each element $T \in \mathcal{T}_h$, from the triangle inequality we have

$$\|\epsilon_b\|_{\partial T} \leq \|\epsilon_0\|_{\partial T} + \|\epsilon_b - \epsilon_0\|_{\partial T}.$$

Thus, it follows from the trace inequality (5.4) that

$$\begin{aligned} \sum_{T \in \mathcal{T}_h} h_T \|\epsilon_b\|_{\partial T}^2 &\leq C \sum_{T \in \mathcal{T}_h} h_T \|\epsilon_0\|_{\partial T}^2 + Ch^2 \sum_{T \in \mathcal{T}_h} h_T^{-1} \|\epsilon_b - \epsilon_0\|_{\partial T}^2 \\ &\leq C(\|\epsilon_0\|^2 + h^2 \|\epsilon_b\|_{W_h}^2), \end{aligned}$$

which, together with the error estimates (5.7) and (6.9), completes the proof of the theorem. \square

7. Numerical Experiments. The primal dual weak Galerkin finite element scheme (2.4)-(2.5) has been implemented for the case of $k = 1$ and $k = 2$ respectively. The objective of this section is to report some of the computational results.

For $k = 1$, the numerical primal variable λ_h and the dual variable u_h are obtained from the following finite element spaces:

$$\begin{aligned} W_h^{(1)} &= \{\lambda_h = \{\lambda_0, \lambda_b\} : \lambda_0 \in P_1(T), \lambda_b \in P_1(e), e \subset \partial T, T \in \mathcal{T}_h\}, \\ M_h^{(1)} &= \{u_h : u_h|_T \in P_0(T), \forall T \in \mathcal{T}_h\}. \end{aligned}$$

For convenience, the corresponding finite element shall be referred to as the $C^{-1} - P_1(T)/P_1(\partial T)/P_0(T)$ element.

For $k = 2$, the finite element spaces for λ_h and u_h are given as follows:

$$\begin{aligned} W_h^{(2)} &= \{\lambda_h = \{\lambda_0, \lambda_b\} : \lambda_0 \in P_2(T), \lambda_b \in P_2(e), e \subset \partial T, T \in \mathcal{T}_h\}, \\ M_h^{(2)} &= \{u_h : u_h|_T \in P_1(T), \forall T \in \mathcal{T}_h\}. \end{aligned}$$

The corresponding finite element shall be referred to as $C^{-1} - P_2(T)/P_2(\partial T)/P_1(T)$ element.

The numerical solutions $\lambda_h = \{\lambda_0, \lambda_b\} \in W_h^{(k)}$ and $u_h \in M_h^{(k)}$ obtained from the PD-WG scheme (2.4)-(2.5) are compared with the L_2 projection of the exact solutions λ and u . Note that u_h approximates the trivial exact solution $u = 0$. The error functions are respectively defined as

$$\epsilon_0 = \lambda_0 - Q_0 \lambda, \quad \epsilon_b = \lambda_b - Q_b \lambda, \quad \text{and} \quad e_h = u_h - Q_h u = u_h.$$

The following L^2 norms are employed to measure the errors:

$$\|\epsilon_0\| = \left(\sum_{T \in \mathcal{T}_h} \int_T \epsilon_0^2 dT \right)^{\frac{1}{2}}, \quad \|\epsilon_b\| = \left(\sum_{T \in \mathcal{T}_h} h_T \int_{\partial T} \epsilon_b^2 ds \right)^{\frac{1}{2}},$$

$$\|e_h\| = \left(\sum_{T \in \mathcal{T}_h} \int_T e_h^2 dT \right)^{\frac{1}{2}}.$$

The numerical experiments are conducted on several polygonal domains; some are convex and the others are non-convex. The domain Ω_1 is convex and is chosen as the unit square $\Omega_1 = (0, 1)^2$. The domain Ω_2 is L-shaped with vertices $A_1 = (0, 0)$, $A_2 = (1, 0)$, $A_3 = (1, 0.5)$, $A_4 = (0.5, 0.5)$, $A_5 = (0.5, 1)$, and $A_6 = (0, 1)$. The third domain is a cracked unit square given by $\Omega_3 = (0, 1)^2 \setminus (0.5, 1) * \{0.5\}$ with a crack along the edge $(0.5, 1) \times \{0.5\}$. The inflow boundary Γ_- is determined by the condition of $\beta \cdot \mathbf{n} < 0$, where \mathbf{n} is the unit outward normal direction to $\partial\Omega$. The right-hand side function f and the inflow Dirichlet boundary data g are chosen to match the exact solution λ if it is known for the test problem.

Uniform triangular and/or rectangular finite element partitions are considered in the numerical tests. The uniform triangulations are generated through a successive uniform refinement of a coarse triangulation of the domain by dividing each coarse triangular element into four congruent sub-triangles by connecting the mid-points on the three edges of the triangular element. The rectangular finite element partitions are generated through a successive uniform refinement of a coarse 3×2 rectangular partition of the domain by dividing each coarse rectangular element into four congruent sub-rectangles by connecting the mid-points on the two parallel edges of the rectangular element respectively.

7.1. Constant-valued convection vector β . This test problem assumes the domain is Ω_1 , the exact solution is given by $\lambda = \cos(x) \cos(y)$, the convection tensor is $\beta = [1, 1]$, and the reaction coefficient is $c = 1$. Tables 7.1-7.6 illustrate the numerical performance of the $C^{-1} - P_1(T)/P_1(\partial T)/P_0(T)$ element when triangular and rectangular partitions are employed. The numerical results in Tables 7.1-7.2 suggest that the convergence rates for ϵ_0 and ϵ_b in the discrete L^2 norm are a bit higher than the optimal order of $\mathcal{O}(h^2)$ with the parameter value $(\tau_1, \tau_2) = (1, 1)$ and $(\tau_1, \tau_2) = (0, 1)$ respectively. The numerical results clearly outperform what the theory predicts. Tables 7.4-7.5 indicate that the convergence rates for ϵ_0 and ϵ_b in the discrete L^2 norm are of order $\mathcal{O}(h^2)$ for the parameters $(\tau_1, \tau_2) = (1, 1)$ and $(\tau_1, \tau_2) = (0, 1)$ respectively, which are in good consistency with the theory. Tables 7.3 and 7.6 illustrate the convergence rates for ϵ_0 and ϵ_b in the discrete L^2 norm seem to reach an optimal order of $\mathcal{O}(h^2)$ for the parameters $(\tau_1, \tau_2) = (0, 0)$. Note that the theory established in Theorems 6.4-6.5 is not applicable to the case $\tau_2 = 0$.

TABLE 7.1

Numerical rates of convergence for the $C^{-1} - P_1(T)/P_1(\partial T)/P_0(T)$ element with the exact solution $\lambda = \cos(x)\cos(y)$ on the unit square domain Ω_1 ; uniform triangular partitions; convection vector $\beta = [1, 1]$; reaction coefficient $c = 1$; and the parameters $(\tau_1, \tau_2) = (1, 1)$.

$1/h$	$\ \epsilon_0\ $	order	$\ \epsilon_b\ $	order	$\ e_h\ $	order
1	2.0109E-01		3.9891E-01		3.0140E-03	
2	6.2996E-02	1.6745	1.1303E-01	1.8193	6.9918E-03	-1.2140
4	1.7817E-02	1.8220	2.9561E-02	1.9350	9.2100E-03	-0.3975
8	3.8874E-03	2.1964	6.0574E-03	2.2869	5.3950E-03	0.7716
16	8.1581E-04	2.2525	1.2029E-03	2.3321	2.2502E-03	1.2616
32	1.8214E-04	2.1632	2.5723E-04	2.2254	8.9122E-04	1.3362

TABLE 7.2

Numerical rates of convergence for the $C^{-1} - P_1(T)/P_1(\partial T)/P_0(T)$ element with the exact solution $\lambda = \cos(x)\cos(y)$ on the unit square domain Ω_1 ; uniform triangular partitions; convection vector $\beta = [1, 1]$; reaction coefficient $c = 1$; and the parameters $(\tau_1, \tau_2) = (0, 1)$.

$1/h$	$\ \epsilon_0\ $	order	$\ \epsilon_b\ $	order	$\ e_h\ $	order
1	2.1739E-01		4.3538E-01		8.0772E-03	
2	5.7342E-02	1.9227	1.0650E-01	2.0313	1.4788E-02	-0.8725
4	1.2879E-02	2.1546	2.2656E-02	2.2329	1.0705E-02	0.4661
8	2.7182E-03	2.2443	4.6597E-03	2.2816	5.9136E-03	0.8562
16	5.9160E-04	2.1999	1.0064E-03	2.2111	3.0013E-03	0.9784
32	1.3639E-04	2.1169	2.3136E-04	2.1210	1.5008E-03	0.9999

TABLE 7.3

Numerical rates of convergence for the $C^{-1} - P_1(T)/P_1(\partial T)/P_0(T)$ element with the exact solution $\lambda = \cos(x)\cos(y)$ on the unit square domain Ω_1 ; uniform triangular partitions; convection vector $\beta = [1, 1]$; reaction coefficient $c = 1$; and the parameters $(\tau_1, \tau_2) = (0, 0)$.

$1/h$	$\ \epsilon_0\ $	order	$\ \epsilon_b\ $	order	$\ e_h\ $	order
1	1.9486E-01		3.9282E-01		1.7572E-02	
2	4.6577E-02	2.0648	8.9249E-02	2.1380	1.7877E-02	-0.0248
4	1.0883E-02	2.0976	1.9684E-02	2.1808	1.1270E-02	0.6656
8	2.4728E-03	2.1379	4.3116E-03	2.1908	5.9859E-03	0.9128
16	5.6872E-04	2.1203	9.7480E-04	2.1450	3.0096E-03	0.9920
32	1.3458E-04	2.0793	2.2889E-04	2.0904	1.5017E-03	1.0030

TABLE 7.4

Numerical rates of convergence for the $C^{-1} - P_1(T)/P_1(\partial T)/P_0(T)$ element with the exact solution $\lambda = \cos(x)\cos(y)$ on the unit square domain Ω_1 ; uniform rectangular partitions; convection vector $\beta = [1, 1]$; reaction coefficient $c = 1$; and the parameters $(\tau_1, \tau_2) = (1, 1)$.

$1/h$	$\ \epsilon_0\ $	order	$\ \epsilon_b\ $	order	$\ e_h\ $	order
1	5.7715E-02		1.7065E-01		3.3964E-02	
2	1.7618E-02	1.7119	4.3922E-02	1.9580	6.5677E-03	2.3706
4	5.2857E-03	1.7368	1.1482E-02	1.9355	1.8300E-03	1.8435
8	1.3192E-03	2.0024	2.5935E-03	2.1465	8.3184E-04	1.1375
16	3.1970E-04	2.0449	5.8821E-04	2.1405	3.2740E-04	1.3453
32	7.8030E-05	2.0346	1.3792E-04	2.0926	1.1616E-04	1.4949

TABLE 7.5

Numerical rates of convergence for the $C^{-1} - P_1(T)/P_1(\partial T)/P_0(T)$ element with the exact solution $\lambda = \cos(x)\cos(y)$ on the unit square domain Ω_1 ; uniform rectangular partitions; convection vector $\beta = [1, 1]$; reaction coefficient $c = 1$; and the parameters $(\tau_1, \tau_2) = (0, 1)$.

$1/h$	$\ \epsilon_0\ $	order	$\ \epsilon_b\ $	order	$\ e_h\ $	order
1	9.5831E-02		2.6881E-01		1.4294E-03	
2	2.0168E-02	2.2484	4.9829E-02	2.4315	2.2216E-03	-0.6362
4	5.4250E-03	1.8944	1.1816E-02	2.0761	1.8549E-03	0.2603
8	1.3251E-03	2.0335	2.6149E-03	2.1760	8.9745E-04	1.0475
16	3.1991E-04	2.0504	5.9016E-04	2.1476	3.3792E-04	1.4092
32	7.8039E-05	2.0354	1.3815E-04	2.0948	1.1614E-04	1.5408

TABLE 7.6

Numerical rates of convergence for the $C^{-1} - P_1(T)/P_1(\partial T)/P_0(T)$ element with the exact solution $\lambda = \cos(x)\cos(y)$ on the unit square domain Ω_1 ; uniform rectangular partitions; convection vector $\beta = [1, 1]$; reaction coefficient $c = 1$; and the parameters $(\tau_1, \tau_2) = (0, 0)$.

$1/h$	$\ \epsilon_0\ $	order	$\ \epsilon_b\ $	order	$\ e_h\ $	order
1	9.5230E-02		2.6695E-01		1.5187E-03	
2	1.9874E-02	2.2605	4.9013E-02	2.4453	2.2637E-03	-0.5758
4	5.3456E-03	1.8945	1.1620E-02	2.0765	1.8751E-03	0.2718
8	1.3145E-03	2.0238	2.5890E-03	2.1661	9.0089E-04	1.0575
16	3.1893E-04	2.0432	5.8772E-04	2.1392	3.3841E-04	1.4126
32	7.7962E-05	2.0324	1.3796E-04	2.0909	1.1621E-04	1.5420

Tables 7.7 - 7.9 present the numerical performance of $C^{-1} - P_1(T)/P_1(\partial T)/P_0(T)$ element for the uniform triangular partition on the non-convex L-shaped domain Ω_2 . The exact solution is $\lambda = \cos(x)\cos(y)$; the convection vector is $\beta = [1, 1]$; and the reaction coefficient is $c = 1$. The parameters are taken as $(\tau_1, \tau_2) = (1, 1)$, $(\tau_1, \tau_2) = (0, 1)$, and $(\tau_1, \tau_2) = (0, 0)$, respectively. Tables 7.7 - 7.9 show that the convergence order for ϵ_0 and ϵ_b in the discrete L^2 norm arrives at the optimal order of $\mathcal{O}(h^2)$.

TABLE 7.7

Numerical rates of convergence for the $C^{-1} - P_1(T)/P_1(\partial T)/P_0(T)$ element with the exact solution $\lambda = \cos(x)\cos(y)$ on the L-shaped domain Ω_2 ; uniform triangular partitions; convection vector $\beta = [1, 1]$; reaction coefficient $c = 1$; and the parameters $(\tau_1, \tau_2) = (1, 1)$.

$1/h$	$\ \epsilon_0\ $	order	$\ \epsilon_b\ $	order	$\ e_h\ $	order
1	3.1337E-02		5.7371E-02		5.4743E-03	
2	8.5496E-03	1.8739	1.4445E-02	1.9897	4.4327E-03	0.3045
4	2.1599E-03	1.9849	3.3992E-03	2.0873	3.6959E-03	0.2622
8	4.5758E-04	2.2389	6.5979E-04	2.3651	1.8038E-03	1.0349
16	1.0559E-04	2.1155	1.4455E-04	2.1904	6.9255E-04	1.3810
32	2.5279E-05	2.0625	3.3466E-05	2.1109	2.9068E-04	1.2525

TABLE 7.8

Numerical rates of convergence for the $C^{-1} - P_1(T)/P_1(\partial T)/P_0(T)$ element with the exact solution $\lambda = \cos(x)\cos(y)$ on the L-shaped domain Ω_2 ; uniform triangular partitions; convection vector $\beta = [1, 1]$; reaction coefficient $c = 1$; and the parameters $(\tau_1, \tau_2) = (0, 1)$.

$1/h$	$\ \epsilon_0\ $	order	$\ \epsilon_b\ $	order	$\ e_h\ $	order
1	2.9300E-02		5.9166E-02		1.2609E-02	
2	6.1821E-03	2.2448	1.2359E-02	2.2592	8.2409E-03	0.6136
4	1.3211E-03	2.2264	2.6236E-03	2.2359	4.6023E-03	0.8404
8	2.6988E-04	2.2913	5.5781E-04	2.2337	2.3407E-03	0.9754
16	6.2113E-05	2.1194	1.3109E-04	2.0892	1.1693E-03	1.0013
32	1.4693E-05	2.0798	3.1540E-05	2.0553	5.8499E-04	0.9991

TABLE 7.9

Numerical rates of convergence for the $C^{-1} - P_1(T)/P_1(\partial T)/P_0(T)$ element with the exact solution $\lambda = \cos(x)\cos(y)$ on the L-shaped domain Ω_2 ; uniform triangular partitions; convection vector $\beta = [1, 1]$; reaction coefficient $c = 1$; and the parameters $(\tau_1, \tau_2) = (0, 0)$.

$1/h$	$\ \epsilon_0\ $	order	$\ \epsilon_b\ $	order	$\ e_h\ $	order
1	2.8906E-02		5.8716E-02		1.3434E-02	
2	6.1177E-03	2.2403	1.2295E-02	2.2557	8.3837E-03	0.6803
4	1.3091E-03	2.2244	2.6101E-03	2.2359	4.6248E-03	0.8582
8	2.6892E-04	2.2834	5.5695E-04	2.2285	2.3432E-03	0.9809
16	6.2049E-05	2.1157	1.3104E-04	2.0875	1.1696E-03	1.0025
32	1.4888E-05	2.0592	3.1537E-05	2.0549	5.8502E-04	0.9994

In Tables 7.10-7.15, we demonstrate the numerical performance of the $C^{-1} - P_2(T)/P_2(\partial T)/P_1(T)$ element on uniform triangular partitions of the unit square domain Ω_1 and the L-shaped domain Ω_2 , respectively. The exact solution is $\lambda = \cos(x)\cos(y)$; the convection vector is $\beta = [1, 1]$; and the reaction coefficient is $c = 1$. The numerical results show that the convergence rates for ϵ_0 and ϵ_b in the discrete L^2 norm are of the optimal order $\mathcal{O}(h^3)$ when the parameters are chosen as $(\tau_1, \tau_2) = (1, 1)$, $(\tau_1, \tau_2) = (0, 1)$, and $(\tau_1, \tau_2) = (0, 0)$, respectively.

TABLE 7.10

Numerical rates of convergence for the $C^{-1} - P_2(T)/P_2(\partial T)/P_1(T)$ element with the exact solution $\lambda = \cos(x)\cos(y)$ on the unit square domain Ω_1 ; uniform triangular partitions; convection vector $\beta = [1, 1]$; reaction coefficient $c = 1$; and the parameters $(\tau_1, \tau_2) = (1, 1)$.

$1/h$	$\ \epsilon_0\ $	order	$\ \epsilon_b\ $	order	$\ e_h\ $	order
1	2.2930E-02		3.7827E-02		5.2346E-03	
2	2.7578E-03	3.0556	4.7515E-03	2.9929	1.8394E-03	1.5088
4	3.1406E-04	3.1344	5.5267E-04	3.1039	7.8572E-04	1.2272
8	3.6798E-05	3.0933	6.5190E-05	3.0837	2.2526E-04	1.8024
16	4.4211E-06	3.0572	7.7955E-06	3.0639	5.9157E-05	1.9289
32	5.4026E-07	3.0327	9.4711E-07	3.0410	1.5124E-05	1.9677

TABLE 7.11

Numerical rates of convergence for the $C^{-1} - P_2(T)/P_2(\partial T)/P_1(T)$ element with the exact solution $\lambda = \cos(x)\cos(y)$ on the unit square domain Ω_1 ; uniform triangular partitions; convection vector $\beta = [1, 1]$; reaction coefficient $c = 1$; and the parameters $(\tau_1, \tau_2) = (0, 1)$.

$1/h$	$\ \epsilon_0\ $	order	$\ \epsilon_b\ $	order	$\ e_h\ $	order
1	1.0238E-02		1.9301E-02		3.8199E-04	
2	2.4224E-03	2.0794	4.2489E-03	2.1835	2.3881E-03	-2.6443
4	2.8603E-04	3.0822	5.4886E-04	2.9526	1.0196E-03	1.2278
8	3.1690E-05	3.1741	6.4620E-05	3.0864	3.0835E-04	1.7254
16	3.5243E-06	3.1686	7.5240E-06	3.1024	8.3450E-05	1.8856
32	4.0429E-07	3.1239	8.9192E-07	3.0765	2.1622E-05	1.9484

TABLE 7.12

Numerical rates of convergence for the $C^{-1} - P_2(T)/P_2(\partial T)/P_1(T)$ element with the exact solution $\lambda = \cos(x)\cos(y)$ on the unit square domain Ω_1 ; uniform triangular partitions; convection vector $\beta = [1, 1]$; reaction coefficient $c = 1$; and the parameters $(\tau_1, \tau_2) = (0, 0)$.

$1/h$	$\ \epsilon_0\ $	order	$\ \epsilon_b\ $	order	$\ e_h\ $	order
1	1.0603E-02		1.9936E-02		6.6104E-04	
2	2.8172E-03	1.9122	4.9908E-03	1.9980	3.1747E-03	-2.2638
4	2.9222E-04	3.2691	5.6321E-04	3.1475	1.1058E-03	1.5216
8	3.1924E-05	3.1944	6.5173E-05	3.1113	3.1349E-04	1.8186
16	3.5320E-06	3.1761	7.5429E-06	3.1111	8.3750E-05	1.9042
32	4.0453E-07	3.1262	8.9255E-07	3.0791	2.1640E-05	1.9524

TABLE 7.13

Numerical rates of convergence for the $C^{-1} - P_2(T)/P_2(\partial T)/P_1(T)$ element with the exact solution $\lambda = \cos(x)\cos(y)$ on the L-shaped domain Ω_2 ; uniform triangular partitions; convection vector $\beta = [1, 1]$; reaction coefficient $c = 1$; and the parameters $(\tau_1, \tau_2) = (1, 1)$.

$1/h$	$\ \epsilon_0\ $	order	$\ \epsilon_b\ $	order	$\ e_h\ $	order
1	1.8602E-03		3.1654E-03		2.9270E-03	
2	2.8228E-04	2.7202	5.0711E-04	2.6420	8.2733E-04	1.8229
4	3.4014E-05	3.0529	6.1046E-05	3.0543	2.2506E-04	1.8781
8	4.1542E-06	3.0335	7.4088E-06	3.0426	5.7479E-05	1.9692
16	5.1021E-07	3.0254	9.0482E-07	3.0335	1.4583E-05	1.9787
32	6.3109E-08	3.0152	1.1151E-07	3.0204	3.6764E-06	1.9879

TABLE 7.14

Numerical rates of convergence for the $C^{-1} - P_2(T)/P_2(\partial T)/P_1(T)$ element with the exact solution $\lambda = \cos(x)\cos(y)$ on the L-shaped domain Ω_2 ; uniform triangular partitions; convection vector $\beta = [1, 1]$; reaction coefficient $c = 1$; and the parameters $(\tau_1, \tau_2) = (0, 1)$.

$1/h$	$\ \epsilon_0\ $	order	$\ \epsilon_b\ $	order	$\ e_h\ $	order
1	2.3256E-03		4.3470E-03		2.6712E-03	
2	2.7541E-04	3.0780	5.3573E-04	3.0204	1.0506E-03	1.3463
4	2.9682E-05	3.2140	6.1448E-05	3.1241	3.0201E-04	1.7985
8	3.3257E-06	3.1579	7.1909E-06	3.0951	8.0495E-05	1.9076
16	3.8296E-07	3.1184	8.5521E-07	3.0718	2.0782E-05	1.9536
32	4.5478E-08	3.0740	1.0369E-07	3.0441	5.2789E-06	1.9770

TABLE 7.15

Numerical rates of convergence for the $C^{-1} - P_2(T)/P_2(\partial T)/P_1(T)$ element with the exact solution $\lambda = \cos(x)\cos(y)$ on the L-shaped domain Ω_2 ; uniform triangular partitions; convection vector $\beta = [1, 1]$; reaction coefficient $c = 1$; and the parameters $(\tau_1, \tau_2) = (0, 0)$.

$1/h$	$\ \epsilon_0\ $	order	$\ \epsilon_b\ $	order	$\ e_h\ $	order
1	2.4722E-03		4.6393E-03		2.8720E-03	
2	2.7900E-04	3.1474	5.4309E-04	3.0946	1.0730E-03	1.4204
4	2.9790E-05	3.2274	6.1690E-05	3.1381	3.0360E-04	1.8214
8	3.3289E-06	3.1617	7.1986E-06	3.0993	8.0598E-05	1.9134
16	3.8306E-07	3.1194	8.5546E-07	3.0730	2.0789E-05	1.9549
32	4.5481E-08	3.0742	1.0369E-07	3.0444	5.2794E-04	1.9774

7.2. Continuous convection vector β . The numerical experiments in this subsection assume the exact solution is $\lambda = \exp(x)\cos(y)$, the convection vector is given by $\beta = [0.5 - y, x - 0.5]$; the reaction coefficient is $c = 0$, the parameters are taken as $(\tau_1, \tau_2) = (1, 1)$, $(\tau_1, \tau_2) = (0, 1)$ and $(\tau_1, \tau_2) = (0, 0)$.

Tables 7.16-7.21 show the numerical performance of the $C^{-1} - P_1(T)/P_1(\partial T)/P_0(T)$ element on the uniform triangular partition of the L-shaped domain Ω_2 and the cracked unit square domain Ω_3 , respectively. The numerical results in Tables 7.16-7.21 indicate that the convergence rates for ϵ_0 and ϵ_b in the discrete L^2 norm arrive at the optimal order of $\mathcal{O}(h^2)$, which are consistent with the theory.

TABLE 7.16

Numerical rates of convergence for the $C^{-1} - P_1(T)/P_1(\partial T)/P_0(T)$ element with the exact solution $\lambda = \exp(x)\cos(y)$ on the L-shaped domain Ω_2 ; uniform triangular partitions; convection vector $\beta = [0.5 - y, x - 0.5]$; reaction term $c = 0$; and the parameters $(\tau_1, \tau_2) = (1, 1)$.

$1/h$	$\ \epsilon_0\ $	order	$\ \epsilon_b\ $	order	$\ e_h\ $	order
1	3.2415E-02		6.3078E-02		1.6843E-02	
2	1.1680E-02	1.4726	2.0531E-02	1.6193	2.2578E-02	-0.4228
4	3.1123E-03	1.9080	5.3381E-03	1.9434	2.2642E-02	-0.0041
8	7.3609E-04	2.0800	1.2796E-03	2.0607	1.7348E-02	0.3843
16	1.7703E-04	2.0559	3.1225E-04	2.0349	1.1446E-02	0.6000
32	4.4053E-05	2.0067	7.7975E-05	2.0016	6.9526E-03	0.7192

TABLE 7.17

Numerical rates of convergence for the $C^{-1} - P_1(T)/P_1(\partial T)/P_0(T)$ element with the exact solution $\lambda = \exp(x)\cos(y)$ on the L-shaped domain Ω_2 ; uniform triangular partitions; convection vector $\beta = [0.5 - y, x - 0.5]$; reaction term $c = 0$; and the parameters $(\tau_1, \tau_2) = (0, 1)$.

$1/h$	$\ \epsilon_0\ $	order	$\ \epsilon_b\ $	order	$\ e_h\ $	order
1	1.9423E-02		3.8931E-02		1.8311E-02	
2	1.0108E-02	0.9422	1.7889E-02	1.1219	2.4481E-02	-0.4190
4	3.1700E-03	1.6730	5.4635E-03	1.7112	2.3976E-02	0.0300
8	7.3660E-04	2.1055	1.2945E-03	2.0774	1.8087E-02	0.4067
16	1.7486E-04	2.0746	3.1319E-04	2.0473	1.1790E-02	0.6173
32	4.3373E-05	2.0114	7.8059E-05	2.0044	7.1064E-03	0.7304

TABLE 7.18

Numerical rates of convergence for the $C^{-1} - P_1(T)/P_1(\partial T)/P_0(T)$ element with the exact solution $\lambda = \exp(x)\cos(y)$ on the L-shaped domain Ω_2 ; uniform triangular partitions; convection vector $\beta = [0.5 - y, x - 0.5]$; reaction $c = 0$; and the parameters $(\tau_1, \tau_2) = (0, 0)$.

$1/h$	$\ \epsilon_0\ $	order	$\ \epsilon_b\ $	order	$\ e_h\ $	order
1	6.1648E-02		1.2097E-01		3.9537E-01	
2	1.6157E-02	1.9319	2.9034E-02	2.0588	1.6059E-01	1.2999
4	2.9637E-03	2.4468	5.4408E-03	2.4159	9.2294E-02	0.7991
8	7.1138E-04	2.0587	1.2945E-03	2.0714	4.8769E-02	0.9203
16	1.7444E-04	2.0279	3.1599E-04	2.0345	2.5783E-02	0.9196
32	4.3420E-05	2.0063	7.8403E-05	2.0109	1.3545E-02	0.9287

TABLE 7.19

Numerical rates of convergence for the $C^{-1} - P_1(T)/P_1(\partial T)/P_0(T)$ element with the exact solution $\lambda = \exp(x)\cos(y)$ on the cracked domain Ω_3 ; uniform triangular partitions; convection $\beta = [0.5 - y, x - 0.5]$; reaction $c = 0$; and the parameters $(\tau_1, \tau_2) = (1, 1)$.

$1/h$	$\ \epsilon_0\ $	order	$\ \epsilon_b\ $	order	$\ e_h\ $	order
1	3.3510E-02		6.4966E-02		2.1932E-02	
2	1.2997E-02	1.3665	2.2720E-02	1.5157	2.9850E-02	-0.4447
4	4.8193E-03	1.4312	8.0114E-03	1.5039	3.0696E-02	-0.0403
8	1.6439E-03	1.5517	2.6809E-03	1.5794	2.3851E-02	0.3640
16	4.3889E-04	1.9052	7.1140E-04	1.9140	1.5641E-02	0.6087
32	1.1360E-04	1.9498	1.8362E-04	1.9539	9.4027E-03	0.7342

TABLE 7.20

Numerical rates of convergence for the $C^{-1} - P_1(T)/P_1(\partial T)/P_0(T)$ element with the exact solution $\lambda = \exp(x)\cos(y)$ on the cracked domain Ω_3 ; uniform triangular partitions; convection $\beta = [0.5 - y, x - 0.5]$; reaction $c = 0$; and the parameters $(\tau_1, \tau_2) = (0, 1)$.

$1/h$	$\ \epsilon_0\ $	order	$\ \epsilon_b\ $	order	$\ e_h\ $	order
1	1.9836E-02		3.9620E-02		2.3612E-02	
2	1.1357E-02	0.8046	2.0050E-02	0.9827	3.2625E-02	-0.4664
4	5.2721E-03	1.1071	8.7776E-03	1.1917	3.2435E-02	0.0084
8	1.7029E-03	1.6303	2.7865E-03	1.6554	2.4813E-02	0.3865
16	4.4221E-04	1.9452	7.1948E-04	1.9534	1.6095E-02	0.6245
32	1.1363E-04	1.9604	1.8436E-04	1.9645	9.6079E-03	0.7444

TABLE 7.21

Numerical rates of convergence for the $C^{-1} - P_1(T)/P_1(\partial T)/P_0(T)$ element with the exact solution $\lambda = \exp(x)\cos(y)$ on the cracked domain Ω_3 ; uniform triangular partitions; convection $\beta = [0.5 - y, x - 0.5]$; reaction $c = 0$; and the parameters $(\tau_1, \tau_2) = (0, 0)$.

$1/h$	$\ \epsilon_0\ $	order	$\ \epsilon_b\ $	order	$\ e_h\ $	order
1	1.5431E-01		2.7560E-01		8.0755E-01	
2	3.4877E-02	2.1455	5.9402E-02	2.2140	2.5660E-01	1.6540
4	7.0917E-03	2.2981	1.1811E-02	2.3304	1.4455E-01	0.8280
8	1.8011E-03	1.9772	2.9530E-03	1.9999	7.4987E-02	0.9469
16	4.5484E-04	1.9855	7.4046E-04	1.9957	3.9028E-02	0.9421
32	1.1483E-04	1.9858	1.8634E-04	1.9905	2.0217E-02	0.9490

Tables 7.22-7.27 illustrate the numerical results of the $C^{-1} - P_2(T)/P_2(\partial T)/P_1(T)$ element on the uniform triangular partition of the L-shaped domain Ω_2 and the cracked unit square domain Ω_3 , respectively. The exact solution is given as $\lambda = \exp(x)\cos(y)$; the convection is $\beta = (0.5 - y, x - 0.5)$; and the reaction is $c = 0$. The parameters are given by $(\tau_1, \tau_2) = (1, 1)$, $(\tau_1, \tau_2) = (0, 1)$ and $(\tau_1, \tau_2) = (0, 0)$, respectively. The numerical results in Tables 7.22-7.27 demonstrate that the convergence rates for ϵ_0 and ϵ_b in the discrete L^2 norm arrive at the optimal order of $\mathcal{O}(h^3)$, which are consistent greatly with the theory.

TABLE 7.22

Numerical rates of convergence for the $C^{-1} - P_2(T)/P_2(\partial T)/P_1(T)$ element with the exact solution $\lambda = \exp(x)\cos(y)$ on the L-shaped domain Ω_2 ; uniform triangular partitions; convection $\beta = [0.5 - y, x - 0.5]$; reaction $c = 0$; and the parameters $(\tau_1, \tau_2) = (1, 1)$.

$1/h$	$\ \epsilon_0\ $	order	$\ \epsilon_b\ $	order	$\ e_h\ $	order
1	2.1302E-02		2.6687E-02		1.4892E-02	
2	2.3777E-03	3.1634	3.4624E-03	2.9463	6.4721E-03	1.2023
4	1.3207E-04	4.1702	1.9602E-04	4.1427	1.9829E-03	1.7066
8	9.2125E-06	3.8415	1.4695E-05	3.7376	5.9265E-04	1.7424
16	9.5606E-07	3.2684	1.5840E-06	3.2137	1.7710E-04	1.7427
32	1.1556E-07	3.0484	1.9136E-07	3.0493	5.1634E-05	1.7781

TABLE 7.23

Numerical rates of convergence for the $C^{-1} - P_2(T)/P_2(\partial T)/P_1(T)$ element with the exact solution $\lambda = \exp(x)\cos(y)$ on the L-shaped domain Ω_2 ; uniform triangular partitions; convection $\beta = [0.5 - y, x - 0.5]$; reaction $c = 0$; and the parameters $(\tau_1, \tau_2) = (0, 1)$.

$1/h$	$\ \epsilon_0\ $	order	$\ \epsilon_b\ $	order	$\ e_h\ $	order
1	6.1064E-03		8.2459E-03		3.7357E-03	
2	1.2992E-03	2.2327	1.9879E-03	2.0524	3.2926E-03	0.1822
4	9.3319E-05	3.7993	1.4863E-04	3.7415	1.6764E-03	0.9739
8	8.4882E-06	3.4586	1.4292E-05	3.3784	5.9142E-04	1.5031
16	9.5130E-07	3.1575	1.6239E-06	3.1377	1.8308E-04	1.6917
32	1.1425E-07	3.0578	1.9409E-07	3.0647	5.3445E-05	1.7763

TABLE 7.24

Numerical rates of convergence for the $C^{-1} - P_2(T)/P_2(\partial T)/P_1(T)$ element with the exact solution $\lambda = \exp(x)\cos(y)$ on the L-shaped domain Ω_2 ; uniform triangular partitions; convection $\beta = [0.5 - y, x - 0.5]$; reaction $c = 0$; and the parameters $(\tau_1, \tau_2) = (0, 0)$.

$1/h$	$\ \epsilon_0\ $	order	$\ \epsilon_b\ $	order	$\ e_h\ $	order
1	4.2050E-03		6.9789E-03		7.6006E-02	
2	8.6645E-04	2.2789	1.4333E-03	2.2836	1.7364E-02	2.1300
4	7.7037E-05	3.4915	1.3057E-04	3.4565	4.0621E-03	2.0958
8	8.1542E-06	3.2399	1.4018E-05	3.2195	1.1028E-03	1.8811
16	9.4470E-07	3.1096	1.6197E-06	3.1135	2.9801E-04	1.8877
32	1.1404E-07	3.0503	1.9391E-07	3.0622	7.9925E-05	1.8986

TABLE 7.25

Numerical rates of convergence for the $C^{-1} - P_2(T)/P_2(\partial T)/P_1(T)$ element with the exact solution $\lambda = \exp(x)\cos(y)$ on the cracked domain Ω_3 ; uniform triangular partitions; convection $\beta = [0.5 - y, x - 0.5]$; reaction $c = 0$; and the parameters $(\tau_1, \tau_2) = (1, 1)$.

$1/h$	$\ \epsilon_0\ $	order	$\ \epsilon_b\ $	order	$\ e_h\ $	order
1	2.6589E-02		3.2397E-02		1.8642E-02	
2	2.5601E-03	3.3766	3.6330E-03	3.1566	8.1520E-03	1.1933
4	1.4880E-04	4.1047	2.1653E-04	4.0685	2.5931E-03	1.6525
8	1.0823E-05	3.7813	1.6479E-05	3.7159	7.8293E-04	1.7277
16	1.1555E-06	3.2275	1.7821E-06	3.2090	2.3144E-04	1.7582
32	1.4005E-07	3.0446	2.1456E-07	3.0542	6.6289E-05	1.8038

TABLE 7.26

Numerical rates of convergence for the $C^{-1} - P_2(T)/P_2(\partial T)/P_1(T)$ element with the exact solution $\lambda = \exp(x)\cos(y)$ on the cracked domain Ω_3 ; uniform triangular partitions; convection $\beta = [0.5 - y, x - 0.5]$; reaction $c = 0$; and the parameters $(\tau_1, \tau_2) = (0, 1)$.

$1/h$	$\ \epsilon_0\ $	order	$\ \epsilon_b\ $	order	$\ e_h\ $	order
1	6.4178E-03		8.7544E-03		5.9985E-03	
2	1.3561E-03	2.2426	2.0718E-03	2.0791	4.8223E-03	0.3149
4	1.0909E-04	3.6359	1.6899E-04	3.6159	2.2903E-03	1.0742
8	9.9618E-06	3.4530	1.5845E-05	3.4148	7.9144E-04	1.5330
16	1.1336E-06	3.1355	1.7974E-06	3.1401	2.4064E-04	1.7176
32	1.3714E-07	3.0471	2.1517E-07	3.0624	6.8983E-05	1.8026

TABLE 7.27

Numerical rates of convergence for the $C^{-1} - P_2(T)/P_2(\partial T)/P_1(T)$ element with the exact solution $\lambda = \exp(x)\cos(y)$ on the cracked domain Ω_3 ; uniform triangular partitions; convection $\beta = [0.5 - y, x - 0.5]$; reaction $c = 0$; and the parameters $(\tau_1, \tau_2) = (0, 0)$.

$1/h$	$\ \epsilon_0\ $	order	$\ \epsilon_b\ $	order	$\ e_h\ $	order
1	5.0789E-03		8.3811E-03		8.2058E-02	
2	9.6469E-04	2.3964	1.5700E-03	2.4163	2.0161E-02	2.0251
4	9.1034E-05	3.4056	1.4755E-04	3.4116	4.9032E-03	2.0398
8	9.7249E-06	3.2267	1.5660E-05	3.2360	1.3389E-03	1.8727
16	1.1326E-06	3.1021	1.7997E-06	3.1212	3.6043E-04	1.8933
32	1.3717E-07	3.0456	2.1528E-07	3.0635	9.6096E-05	1.9072

Tables 7.28-7.35 illustrate the numerical results on the uniform triangular partition of the unit square domain Ω_1 . The exact solution is $\lambda = \sin(\pi x)\cos(\pi y)$; the convection is $\beta = [-y, x]$; and the reaction is $c = x + y$. The parameters are given by $(\tau_1, \tau_2) = (0, 1)$, $(\tau_1, \tau_2) = (1, 1)$, $(\tau_1, \tau_2) = (0, 0)$ and $(\tau_1, \tau_2) = (1, 0)$, respectively. The numerical results in Tables 7.28-7.31 demonstrate that the convergence rates for ϵ_0 and ϵ_b in the discrete L^2 norm arrive at the optimal order of $\mathcal{O}(h^2)$ when the $C^{-1} - P_1(T)/P_1(\partial T)/P_0(T)$ element is employed. Tables 7.32-7.35 show that the convergence rates for ϵ_0 and ϵ_b in the discrete L^2 norm are of the optimal order $\mathcal{O}(h^3)$ when the $C^{-1} - P_2(T)/P_2(\partial T)/P_1(T)$ element is used.

TABLE 7.28

Numerical rates of convergence for the $C^{-1} - P_1(T)/P_1(\partial T)/P_0(T)$ element with the exact solution $\lambda = \sin(\pi x) \cos(\pi y)$ on the unit square domain Ω_1 ; uniform triangular partitions; convection $\beta = [-y, x]$; reaction $c = x + y$; and the parameters $(\tau_1, \tau_2) = (0, 1)$.

$1/h$	$\ \epsilon_0\ $	order	$\ \epsilon_b\ $	order	$\ e_h\ $	order
1	2.1635E-00		4.3282E-00		2.9913E-02	
2	6.8925E-01	1.6503	1.2858E-00	1.7511	2.1249E-01	-2.8286
4	1.7782E-01	1.9546	3.1162E-01	2.0448	1.4365E-01	0.5648
8	3.4347E-02	2.3722	5.9643E-02	2.3853	9.7388E-02	0.5608
16	7.8861E-03	2.1228	1.3698E-02	2.1224	5.5483E-02	0.8117
32	1.9449E-03	2.0196	3.3694E-03	2.0234	2.9496E-02	0.9115

TABLE 7.29

Numerical rates of convergence for the $C^{-1} - P_1(T)/P_1(\partial T)/P_0(T)$ element with the exact solution $\lambda = \sin(\pi x) \cos(\pi y)$ on the unit square domain Ω_1 ; uniform triangular partitions; convection $\beta = [-y, x]$; reaction $c = x + y$; and the parameters $(\tau_1, \tau_2) = (1, 1)$.

$1/h$	$\ \epsilon_0\ $	order	$\ \epsilon_b\ $	order	$\ e_h\ $	order
1	2.4003E-00		4.7903E-00		4.9317E-02	
2	6.8303E-01	1.8132	1.2888E-00	1.8941	1.7957E-01	-1.8644
4	1.6889E-01	2.0159	3.0049E-01	2.1001	1.4889E-01	0.2702
8	3.2831E-02	2.3630	5.6977E-02	2.3989	9.5989E-02	0.6333
16	7.7039E-03	2.0914	1.3306E-02	2.0983	5.1431E-02	0.9002
32	1.9429E-03	1.9874	3.3402E-03	1.9941	2.6739E-02	0.9437

TABLE 7.30

Numerical rates of convergence for the $C^{-1} - P_1(T)/P_1(\partial T)/P_0(T)$ element with the exact solution $\lambda = \sin(\pi x) \cos(\pi y)$ on the unit square domain Ω_1 ; uniform triangular partitions; convection $\beta = [-y, x]$; reaction $c = x + y$; and the parameters $(\tau_1, \tau_2) = (0, 0)$.

$1/h$	$\ \epsilon_0\ $	order	$\ \epsilon_b\ $	order	$\ e_h\ $	order
1	3.1677E-00		6.4055E-00		1.2305E-00	
2	6.2169E-01	2.3491	1.176E-00	2.4451	5.0819E-01	1.2758
4	1.3100E-01	2.2466	2.3434E-01	2.3275	2.6253E-01	0.9529
8	3.1142E-02	2.0726	5.4837E-02	2.0954	1.2631E-01	1.0554
16	7.7204E-03	2.0121	1.3469E-02	2.0255	6.1632E-02	1.0353
32	1.9358E-03	1.9957	3.3574E-03	2.0042	3.0642E-02	1.0082

TABLE 7.31

Numerical rates of convergence for the $C^{-1} - P_1(T)/P_1(\partial T)/P_0(T)$ element with the exact solution $\lambda = \sin(\pi x) \cos(\pi y)$ on the unit square domain Ω_1 ; uniform triangular partitions; convection $\beta = [-y, x]$; reaction $c = x + y$; and the parameters $(\tau_1, \tau_2) = (1, 0)$.

$1/h$	$\ \epsilon_0\ $	order	$\ \epsilon_b\ $	order	$\ e_h\ $	order
1	2.7177E-00		5.5313E-00		1.3068E-00	
2	6.8277E-01	1.9929	1.2846E-00	2.1064	6.1251E-01	1.0932
4	1.3531E-01	2.3351	2.4105E-01	2.4139	2.9282E-01	1.0647
8	3.1578E-02	2.0993	5.5178E-02	2.1272	1.2668E-01	1.2089
16	7.7945E-03	2.0184	1.3486E-02	2.0326	5.7844E-02	1.1309
32	1.9530E-03	1.9968	3.3590E-03	2.0054	2.7953E-02	1.0492

TABLE 7.32

Numerical rates of convergence for the $C^{-1} - P_2(T)/P_2(\partial T)/P_1(T)$ element with the exact solution $\lambda = \sin(\pi x) \cos(\pi y)$ on the unit square domain Ω_1 ; uniform triangular partitions; convection $\beta = [-y, x]$; reaction $c = x + y$; and the parameters $(\tau_1, \tau_2) = (0, 1)$.

$1/h$	$\ \epsilon_0\ $	order	$\ \epsilon_b\ $	order	$\ e_h\ $	order
1	8.4480E-01		1.3885E-00		2.6279E-01	
2	1.2875E-01	2.7140	2.1370E-01	2.6999	1.3221E-01	0.9910
4	1.5824E-02	3.0244	2.5988E-02	3.0396	4.6963E-02	1.4933
8	1.4710E-03	3.4272	2.4380E-03	3.4141	1.8782E-02	1.3221
16	1.5733E-04	3.2249	2.5893E-04	3.2351	6.3135E-03	1.5729
32	1.8166E-05	3.1145	2.9573E-05	3.1302	2.0863E-03	1.5975

TABLE 7.33

Numerical rates of convergence for the $C^{-1} - P_2(T)/P_2(\partial T)/P_1(T)$ element with the exact solution $\lambda = \sin(\pi x) \cos(\pi y)$ on the unit square domain Ω_1 ; uniform triangular partitions; convection $\beta = [-y, x]$; reaction $c = x + y$; and the parameters $(\tau_1, \tau_2) = (1, 1)$.

$1/h$	$\ \epsilon_0\ $	order	$\ \epsilon_b\ $	order	$\ e_h\ $	order
1	3.8837E-00		5.4854E-00		5.6478E-01	
2	1.7181E-01	4.4985	2.7930E-01	4.2957	1.5540E-01	1.8617
4	2.4360E-02	2.8183	3.7158E-02	2.9101	5.5710E-02	1.4800
8	1.7514E-03	3.7979	2.8035E-03	3.7284	1.8484E-02	1.5916
16	1.7571E-04	3.3173	2.8321E-04	3.3073	6.2443E-03	1.5657
32	1.9994E-05	3.1355	3.1905E-05	3.1500	2.0630E-02	1.5978

TABLE 7.34

Numerical rates of convergence for the $C^{-1} - P_2(T)/P_2(\partial T)/P_1(T)$ element with the exact solution $\lambda = \sin(\pi x) \cos(\pi y)$ on the unit square domain Ω_1 ; uniform triangular partitions; convection $\beta = [-y, x]$; reaction $c = x + y$; and the parameters $(\tau_1, \tau_2) = (0, 0)$.

$1/h$	$\ \epsilon_0\ $	order	$\ \epsilon_b\ $	order	$\ e_h\ $	order
1	6.9711E-01		1.4242E-00		5.8715E-00	
2	1.7579E-01	1.9875	3.0395E-01	2.2282	1.8269E-00	1.6844
4	1.6556E-02	3.4085	2.7948E-02	3.4430	4.7677E-01	1.9380
8	1.4546E-03	3.5086	2.4227E-03	3.5280	1.2208E-01	1.9654
16	1.5136E-04	3.2646	2.4989E-04	3.2773	3.1089E-02	1.9734
32	1.7656E-05	3.0998	2.8785E-05	3.1179	7.9238E-03	1.9722

TABLE 7.35

Numerical rates of convergence for the $C^{-1} - P_2(T)/P_2(\partial T)/P_1(T)$ element with the exact solution $\lambda = \sin(\pi x) \cos(\pi y)$ on the unit square domain Ω_1 ; uniform triangular partitions; convection $\beta = [-y, x]$; reaction $c = x + y$; and the parameters $(\tau_1, \tau_2) = (1, 0)$.

$1/h$	$\ \epsilon_0\ $	order	$\ \epsilon_b\ $	order	$\ e_h\ $	order
1	1.0306E-00		1.8490E-00		8.8351E-00	
2	1.6984E-01	2.6012	2.9961E-01	2.6256	1.9752E-00	2.1613
4	1.8233E-02	3.2195	3.0485E-02	3.2969	4.8981E-01	2.0117
8	1.6511E-03	3.4651	2.6914E-03	3.5017	1.2298E-01	1.9938
16	1.6687E-04	3.3067	2.7016E-04	3.3165	3.1170E-02	1.9801
32	1.9382E-05	3.1059	3.0957E-05	3.1255	7.9248E-03	1.9757

7.3. Discontinuous convection β . The numerical tests are conducted for the $C^{-1} - P_1(T)/P_1(\partial T)/P_0(T)$ element on uniform triangular partitions of the unit square domain Ω_1 . The exact solution is given by $\lambda = \sin(x) \cos(y)$. The convection $\beta(x, y)$ is piece-wise defined in the sense that $\beta(x, y) = [1, -1]$ for $y < 1 - x$ and $\beta(x, y) = [-2, 2]$ otherwise. The reaction is $c = 1$. The parameters are $(\tau_1, \tau_2) = (1, 1)$, $(\tau_1, \tau_2) = (0, 1)$ and $(\tau_1, \tau_2) = (0, 0)$, respectively. The numerical results in Tables 7.36-7.38 show that the convergence rates for ϵ_0 and ϵ_b in the discrete L^2 norm are of the optimal order $\mathcal{O}(h^2)$, which are consistent with the theory.

TABLE 7.36

Numerical rates of convergence for the $C^{-1} - P_1(T)/P_1(\partial T)/P_0(T)$ element with the exact solution $\lambda = \sin(x) \cos(y)$ on the unit square domain $\Omega_1 = (0, 1)^2$; uniform triangular partitions; convection $\beta = [1, -1]$ for $y < 1 - x$ and $\beta = [-2, 2]$ otherwise; reaction $c = 1$; and the parameters $(\tau_1, \tau_2) = (1, 1)$.

$1/h$	$\ \epsilon_0\ $	order	$\ \epsilon_b\ $	order	$\ e_h\ $	order
1	5.2713E-02		9.8682E-02		3.0619E-03	
2	1.1336E-02	2.2173	2.0662E-02	2.2558	1.5735E-03	0.9604
4	2.7930E-03	2.0210	4.8760E-03	2.0832	9.8137E-04	0.6812
8	6.8883E-04	2.0196	1.1677E-03	2.0620	5.1897E-04	0.9192
16	1.7169E-04	2.0043	2.8597E-04	2.0297	2.6273E-04	0.9820
32	4.2912E-05	2.0004	7.0790E-05	2.0143	1.3186E-04	0.9946

TABLE 7.37

Numerical rates of convergence for the $C^{-1} - P_1(T)/P_1(\partial T)/P_0(T)$ element with exact solution $\lambda = \sin(x)\cos(y)$ on the unit square domain Ω_1 ; uniform triangular partitions; convection $\beta = [1, -1]$ for $y < 1 - x$ and $\beta = [-2, 2]$ otherwise; reaction $c = 1$; and the parameters $(\tau_1, \tau_2) = (0, 1)$.

$1/h$	$\ \epsilon_0\ $	order	$\ \epsilon_b\ $	order	$\ \epsilon_h\ $	order
1	3.2120E-02		7.0574E-02		9.0720E-03	
2	1.1795E-02	1.4452	2.1695E-02	1.7018	2.3864E-03	1.9266
4	2.8507E-03	2.0489	4.9996E-03	2.1175	9.1523E-04	1.3826
8	7.0230E-04	2.0197	1.1936E-03	2.0664	4.2927E-04	1.0922
16	1.7520E-04	2.0045	2.9198E-04	2.0315	2.1125E-04	1.0229
32	4.3771E-05	2.0009	7.2224E-05	2.0153	1.0519E-04	1.0059

TABLE 7.38

Numerical rates of convergence for the $C^{-1} - P_1(T)/P_1(\partial T)/P_0(T)$ element with the exact solution $\lambda = \sin(x)\cos(y)$ on the unit square domain Ω_1 ; uniform triangular partitions; convection $\beta = [1, -1]$ for $y < 1 - x$ and $\beta = [-2, 2]$ otherwise; reaction $c = 1$; and the parameters $(\tau_1, \tau_2) = (0, 0)$.

$1/h$	$\ \epsilon_0\ $	order	$\ \epsilon_b\ $	order	$\ \epsilon_h\ $	order
1	4.0936E-02		9.0019E-02		1.3976E-02	
2	1.2259E-02	1.7396	2.2582E-02	1.9951	3.0632E-03	2.1899
4	2.9157E-03	2.0719	5.1131E-03	2.1429	1.2530E-03	1.2896
8	7.1768E-04	2.0224	1.2183E-03	2.0693	5.9790E-04	1.0675
16	1.7876E-04	2.0053	2.9787E-04	2.0321	2.9519E-04	1.0183
32	4.4655E-05	2.0012	7.3676E-05	2.0154	1.4707E-04	1.0051

Figures 7.1-7.2 illustrate the plots of the numerical solution λ_0 arising from the PD-WG scheme (2.4)-(2.5) when the $C^{-1} - P_1(T)/P_1(\partial T)/P_0(T)$ element and the $C^{-1} - P_2(T)/P_2(\partial T)/P_1(T)$ element are employed, respectively. Uniform triangular partitions are employed in the numerical experiments on the unit square domain Ω_1 . The configuration of the test problem is as follows: (1) the convection is piece-wisely defined in the sense that $\beta(x, y) = [1, -1]$ for $y < 1 - x$ and $\beta(x, y) = [-2, 2]$ elsewhere; (2) the reaction is $c = 0$; (3) the load function is $f = 0$; and (4) the inflow boundary data is given by $g = 1$ on the inflow boundary edge $\{0\} * (0, 1)$ and by $g = -1$ on the inflow boundary edge $\{1\} * (0, 1)$. The parameters are given by $(\tau_1, \tau_2) = (1, 1)$. The left ones in Figures 7.1-7.2 present the contour plots of the numerical solution λ_0 ; and the right ones demonstrate the surface plots for the numerical solution λ_0 . It is easy to see that the numerical solution λ_0 arising from the PD-WG scheme (2.4)-(2.5) is consistent with the exact solution λ of the model problem (1.1) in this test problem.

7.4. Plots for numerical solution λ_0 when the exact solution λ is unknown. Figures 7.3-7.4 show the contour plots of the numerical solution λ_0 on the uniform triangular partition of the unit square domain Ω_1 when the $C^{-1} - P_1(T)/P_1(\partial T)/P_0(T)$ element and the $C^{-1} - P_2(T)/P_2(\partial T)/P_1(T)$ element are employed respectively. The configuration of this test problem is as follows: the convection vector $\beta = [0.5 - y, x - 0.5]$, the reaction $c = 1$, the inflow boundary data $g = \cos(5y)$, and the parameters $(\tau_1, \tau_2) = (1, 1)$. The left ones and the right ones in Figures 7.3-7.4 demonstrate the contour plots of the numerical solution λ_0 corresponding to the load function $f = 1$ and the load function $f = 0$, respectively.

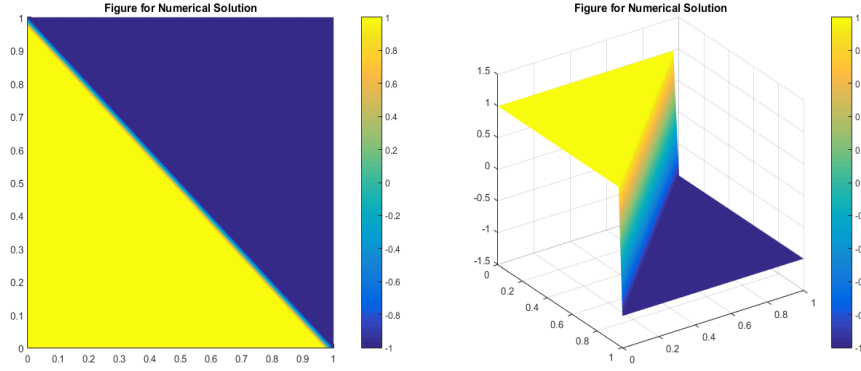


FIG. 7.1. Plots of numerical solution λ_0 on the unit square domain Ω_1 ; $C^{-1} - P_1(T)/P_1(\partial T)/P_0(T)$ element; uniform triangular partitions; convection $\beta = [1, -1]$ for $y < 1 - x$ and $\beta = [-2, 2]$ elsewhere; reaction $c = 0$; the load function $f = 0$; the inflow boundary data $g = 1$ on the inflow boundary edge $\{0\} * (0, 1)$ and $g = -1$ on the inflow boundary edge $\{1\} * (0, 1)$; and $(\tau_1, \tau_2) = (1, 1)$. Contour plot (left); surface plot (right).

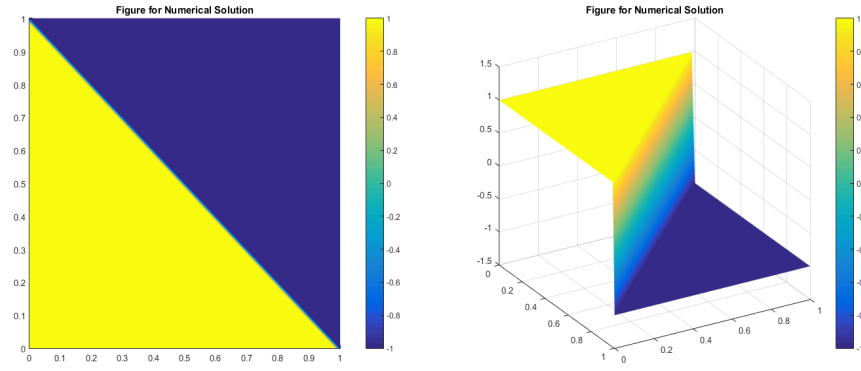


FIG. 7.2. Plots of numerical solution λ_0 on the unit square domain Ω_1 ; $C^{-1} - P_2(T)/P_2(\partial T)/P_1(T)$ element; uniform triangular partitions; convection $\beta = [1, -1]$ for $y < 1 - x$ and $\beta = [-2, 2]$ elsewhere; reaction $c = 0$; the load function $f = 0$; the inflow boundary data $g = 1$ on the inflow boundary edge $\{0\} * (0, 1)$ and $g = -1$ on the inflow boundary edge $\{1\} * (0, 1)$; and $(\tau_1, \tau_2) = (1, 1)$. Contour plot (left); surface plot (right).

Figures 7.5-7.6 show the contour plots of the numerical solution λ_0 on the uniform triangular partition of the unit square domain Ω_1 for the $C^{-1} - P_1(T)/P_1(\partial T)/P_0(T)$ element and the $C^{-1} - P_2(T)/P_2(\partial T)/P_1(T)$ element respectively. The convection vector is piece-wisely defined in the sense that $\beta(x, y) = [-y, x]$ for $y < 1 - x$ and $\beta(x, y) = [1 - y, x - 1]$ otherwise. The reaction is $c = 0$. The inflow boundary data is given by $g = \sin(3x) \cos(5y)$. The parameters are $(\tau_1, \tau_2) = (1, 1)$. Figures 7.5-7.6 demonstrate the contour plots of the numerical solution λ_0 for the load function $f = 1$ (left figures) and the load function $f = 0$ (right figures), respectively.

Figures 7.7-7.8 show the contour plots of the numerical solution λ_0 on the uniform triangular partition of the L-shaped domain Ω_2 . The convection vector is piece-wisely given by $\beta(x, y) = [-1, 1]$ for $y < 0.5 - x$ and $\beta(x, y) = [1, -1]$ elsewhere. The

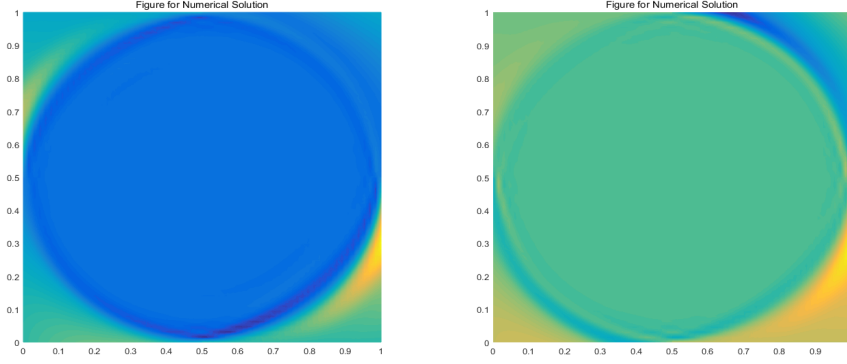


FIG. 7.3. Contour plots of numerical solution λ_0 on the unit square domain Ω_1 ; $C^{-1} - P_1(T)/P_1(\partial T)/P_0(T)$ element; uniform triangular partitions; the convection $\beta = [0.5 - y, x - 0.5]$; the reaction $c = 1$; the inflow boundary data $g = \cos(5y)$; and $(\tau_1, \tau_2) = (1, 1)$. The load function $f = 1$ (left); the load function $f = 0$ (right).

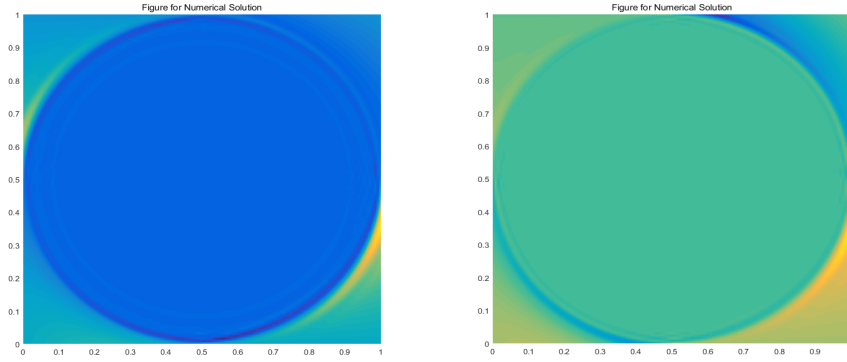


FIG. 7.4. Contour plots of numerical solution λ_0 on the unit square domain Ω_1 ; $C^{-1} - P_2(T)/P_2(\partial T)/P_1(T)$ element; uniform triangular partitions; convection $\beta = [0.5 - y, x - 0.5]$; reaction $c = 1$; the inflow boundary data $g = \cos(5y)$; and $(\tau_1, \tau_2) = (1, 1)$. The load function $f = 1$ (left); the load function $f = 0$ (right).

reaction is $c = 1$. The inflow boundary data is $g = \sin(\pi x) \cos(\pi y)$. The parameters are set as $(\tau_1, \tau_2) = (1, 1)$. Figure 7.7 demonstrates the contour plots of the numerical solution λ_0 for the load functions $f = 1$ and $f = 0$ respectively when the $C^{-1} - P_1(T)/P_1(\partial T)/P_0(T)$ element is employed. Figure 7.8 illustrates the contour plots of the numerical solution λ_0 for the load functions $f = 1$ and $f = 0$ respectively when the $C^{-1} - P_2(T)/P_2(\partial T)/P_1(T)$ element is used.

Figures 7.9-7.10 show the contour plots of the numerical solution λ_0 on the uniform triangular partition of the cracked unit square domain Ω_3 . The convection vector is given by $\beta = [0.5 - y, x - 0.5]$; the reaction is $c = x - y$; the inflow boundary data is $g = \sin(x)$; and the parameters are $(\tau_1, \tau_2) = (1, 1)$. Figures 7.9-7.10 demonstrate the contour plots of the numerical solution λ_0 for the load function $f = 1$ (left ones) and the load function $f = 0$ (right ones) when the $C^{-1} - P_1(T)/P_1(\partial T)/P_0(T)$ element

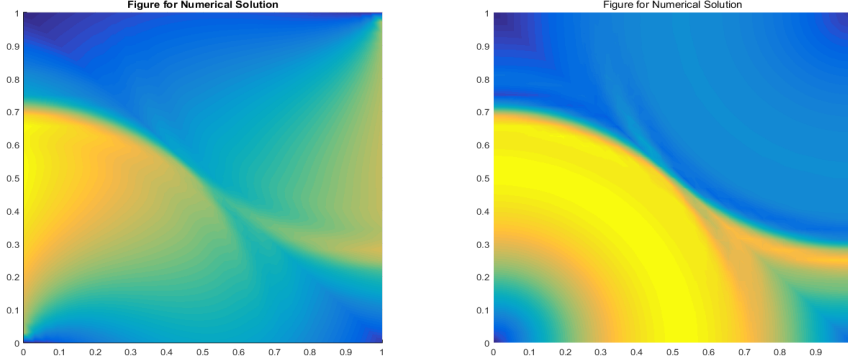


FIG. 7.5. Contour plots of numerical solution λ_0 on the unit square domain Ω_1 ; $C^{-1} - P_1(T)/P_1(\partial T)/P_0(T)$ element; uniform triangular partitions; convection $\beta = [-y, x]$ for $y < 1 - x$ and $\beta = [1 - y, x - 1]$ otherwise; reaction $c = 0$; the inflow boundary data $g = \sin(3x)\cos(5y)$; and $(\tau_1, \tau_2) = (1, 1)$. The load function $f = 1$ (left); the load function $f = 0$ (right).

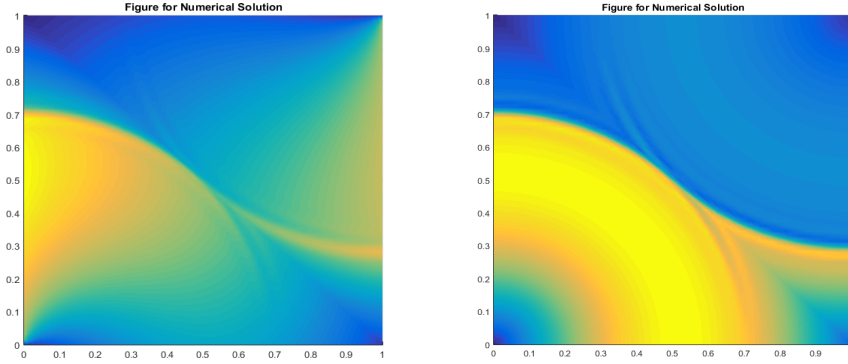


FIG. 7.6. Contour plots of numerical solution λ_0 on the unit square domain Ω_1 ; $C^{-1} - P_2(T)/P_2(\partial T)/P_1(T)$ element; uniform triangular partitions; convection $\beta = [-y, x]$ for $y < 1 - x$ and $\beta = [1 - y, x - 1]$ otherwise; reaction $c = 0$; the inflow boundary data $g = \sin(3x)\cos(5y)$; and $(\tau_1, \tau_2) = (1, 1)$. The load function $f = 1$ (left); the load function $f = 0$ (right).

and the $C^{-1} - P_2(T)/P_2(\partial T)/P_1(T)$ element are employed respectively.

In summary, the numerical performance of the primal-dual weak Galerkin scheme (2.4)-(2.5) for solving the first-order linear convection problem (1.1) is consistent with the theory developed in this paper. The numerical results reveal optimal-order of convergence for all the test problems. We are confident that the PD-WG scheme is a stable, accurate, and convergent numerical method for the first-order linear convection problem in non-divergence form.

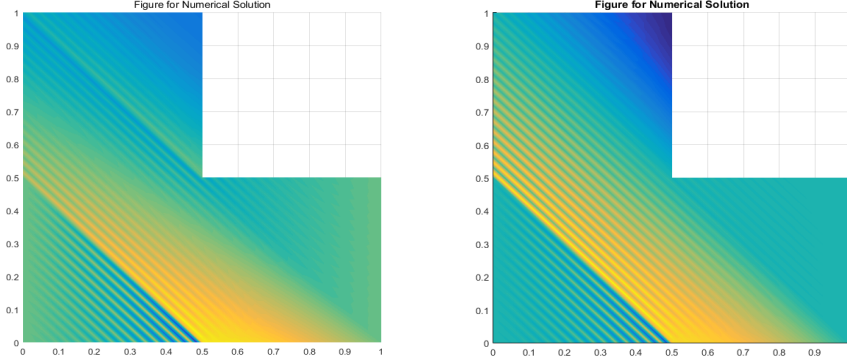


FIG. 7.7. Contour plots of numerical solution λ_0 on the L-shaped domain Ω_2 ; $C^{-1} - P_1(T)/P_1(\partial T)/P_0(T)$ element; uniform triangular partitions; convection vector $\beta = [-1, 1]$ for $y < 0.5 - x$ and $\beta = [1, -1]$ elsewhere; reaction $c = 1$; the inflow boundary data $g = \sin(\pi x) \cos(\pi y)$; and $(\tau_1, \tau_2) = (1, 1)$. The load function $f = 1$ (left); the load function $f = 0$ (right).

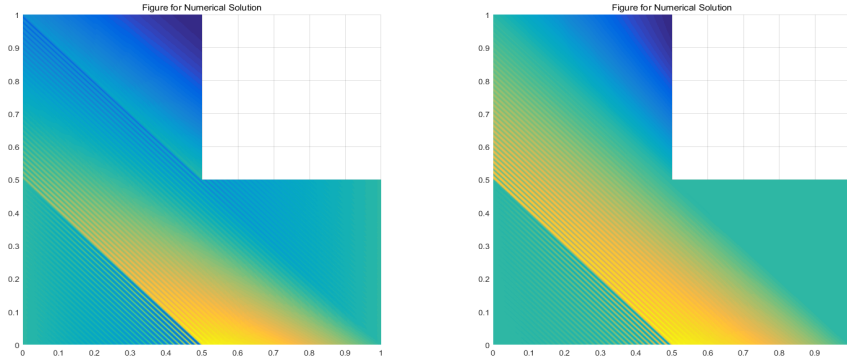


FIG. 7.8. Contour plots of numerical solution λ_0 on the L-shaped domain Ω_2 ; $C^{-1} - P_2(T)/P_2(\partial T)/P_1(T)$ element; uniform triangular partitions; convection $\beta = [-1, 1]$ for $y < 0.5 - x$ and $\beta = [1, -1]$ elsewhere; reaction $c = 1$; the inflow boundary data $g = \sin(\pi x) \cos(\pi y)$; and $(\tau_1, \tau_2) = (1, 1)$. The load function $f = 1$ (left); the load function $f = 0$ (right).

REFERENCES

- [1] I. BABUŠKA, *The finite element method with Lagrange multipliers*, Numer. Math., vol. 20, pp. 179-192, 1973.
- [2] E. BURMAN, *Stabilized finite element methods for nonsymmetric, noncoercive, and ill-posed problems. Part I: Elliptic equations*, SIAM J. Sci. Comput., vol. 35, No. 6, pp. A2752-A2780, 2013.
- [3] E. BURMAN, *Stabilized finite element methods for nonsymmetric, noncoercive, and ill-posed problems. Part II: hyperbolic equations*, SIAM J. Sci. Comput., vol. 36, No. 4, pp. A1911-A1936, 2014.
- [4] C. WANG, AND J. WANG, *A primal-dual weak Galerkin finite element method for second order elliptic equations in non-divergence form*, Math. Comp., vol. 87, pp. 515-545, 2018.
- [5] C. WANG, *A New Primal-Dual Weak Galerkin Finite Element Method for Ill-posed Elliptic Cauchy Problems*, arXiv:1809.04697.
- [6] C. WANG, AND J. WANG, *A Primal-Dual weak Galerkin finite element method for Fokker-*

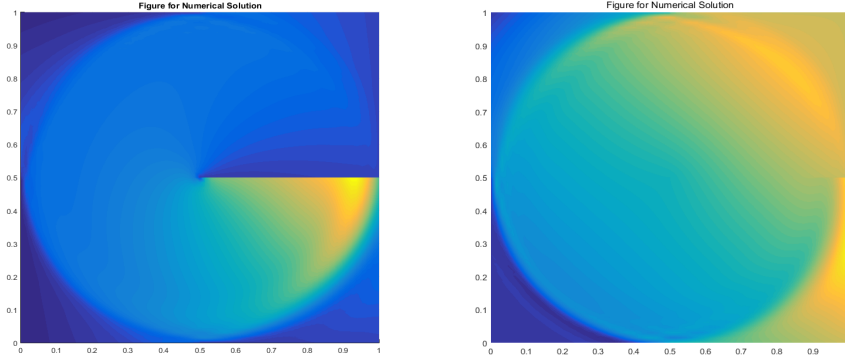


FIG. 7.9. Contour plots of numerical solution λ_0 on the cracked square domain Ω_3 ; $C^{-1} - P_1(T)/P_1(\partial T)/P_0(T)$ element; uniform triangular partitions; convection $\beta = [0.5 - y, x - 0.5]$; reaction $c = x - y$; the inflow boundary data $g = \sin(x)$; and $(\tau_1, \tau_2) = (1, 1)$. The load function $f = 1$ (left); the load function $f = 0$ (right).

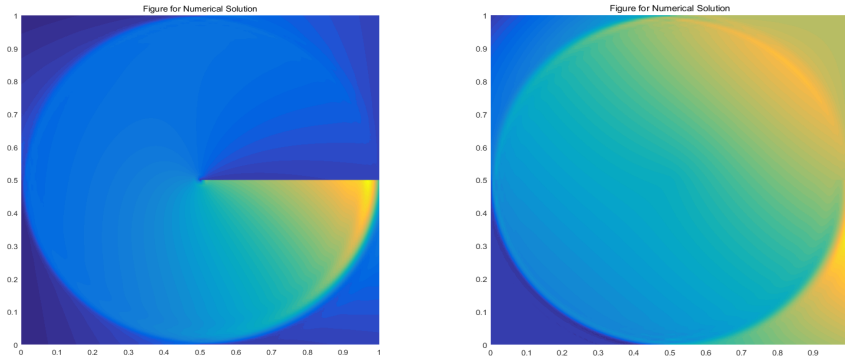


FIG. 7.10. Contour plots of numerical solution λ_0 on the cracked square domain Ω_3 ; $C^{-1} - P_2(T)/P_2(\partial T)/P_1(T)$ element; uniform triangular partitions; convection $\beta = [0.5 - y, x - 0.5]$; reaction $c = x - y$; the inflow boundary data $g = \sin(x)$; and $(\tau_1, \tau_2) = (1, 1)$. The load function $f = 1$ (left); the load function $f = 0$ (right).

Planck type equations, arXiv:1704.05606.

- [7] C. WANG, AND J. WANG, *Primal-Dual Weak Galerkin Finite Element Methods for Elliptic Cauchy Problems*, Computers and Mathematics with Applications, vol. 78, pp. 905-928, 2019.
- [8] C. WANG, AND J. WANG, *A primal-dual finite element method for first-order transport problems*, arXiv. 1906.07336.
- [9] J. WANG AND X. YE, *A weak Galerkin mixed finite element method for second-order elliptic problems*, Math. Comp., vol. 83, pp. 2101-2126, 2014.
- [10] C. WANG, AND L. ZIKATANOV, *Low Regularity Primal-Dual Weak Galerkin Finite Element Methods for Convection-Diffusion Equations*, arXiv:1901.06743.